Outline: Future UNILAC experiments

Lecturer: Hans-Jürgen Wollersheim

e-mail: h.j.wollersheim@gsi.de

web-page: https://web-docs.gsi.de/~wolle/ and click on

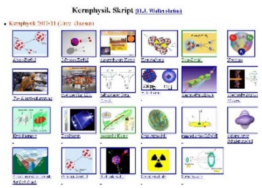

1. Coulomb excitation
2. α-transfer reaction
3. electron spectroscopy
4. K-isomerism
5. transient magnetic field
6. spectroscopy of fission fragments

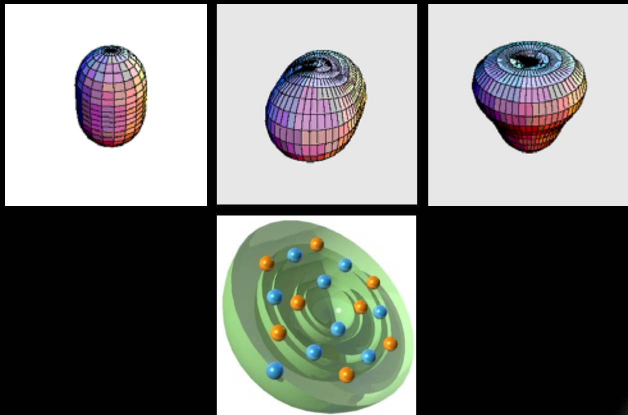

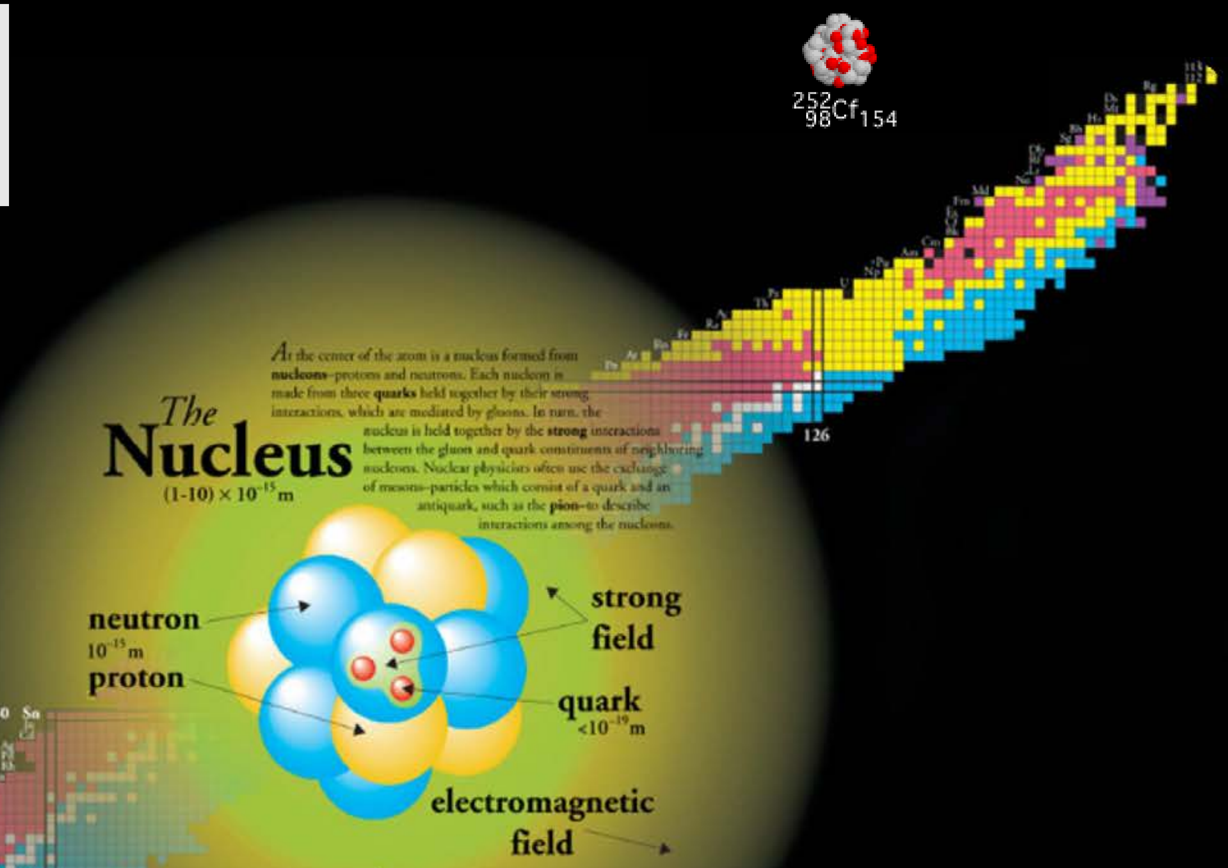

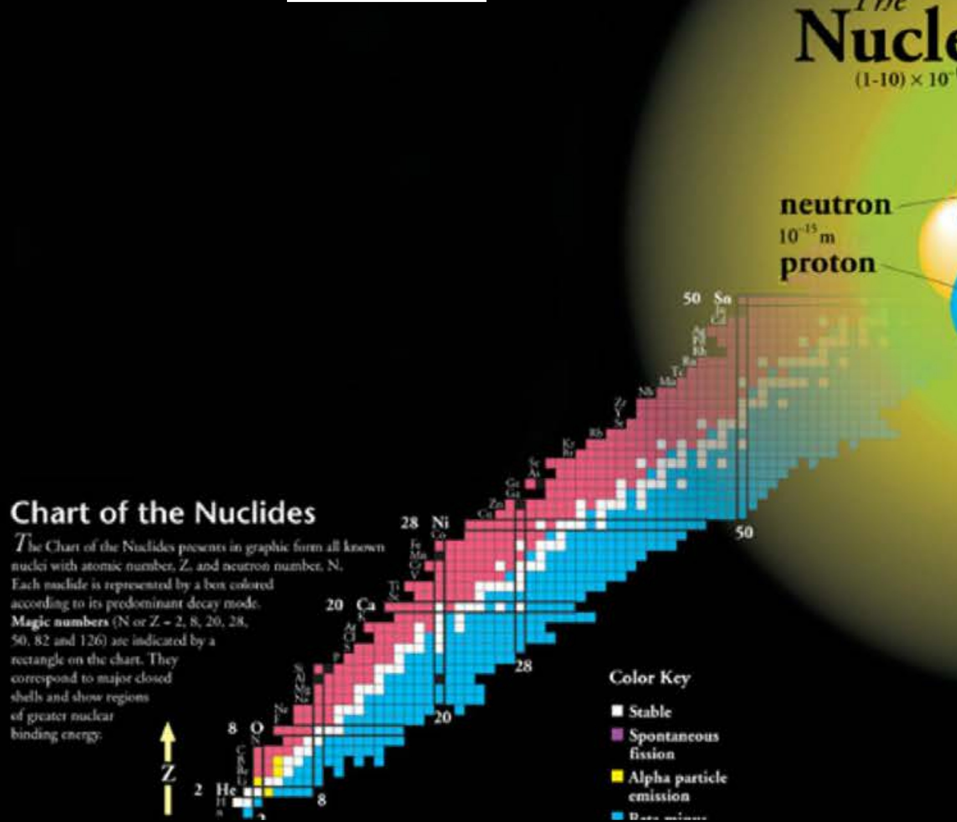

heavy ion
nuclear reactions

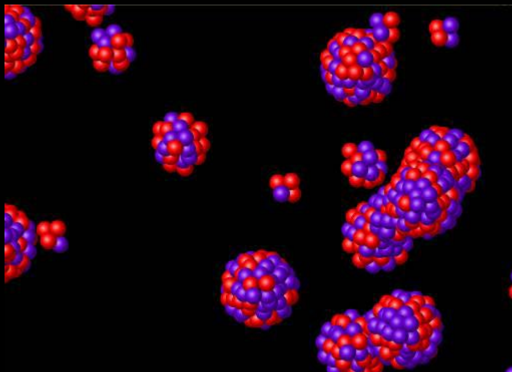

Heavy ion nuclear reactions

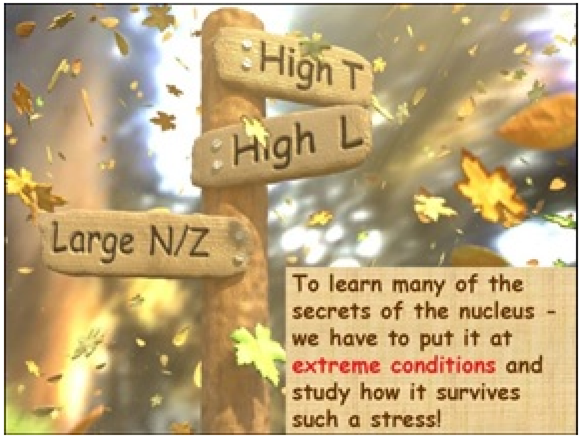

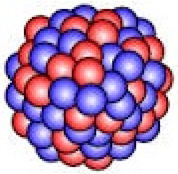

SIS-18

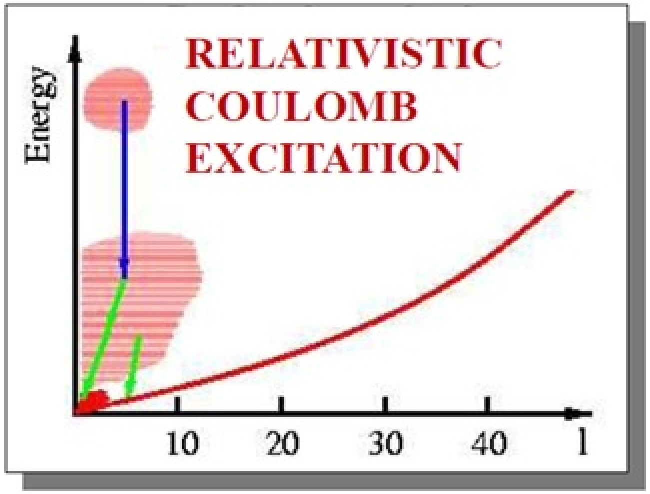

UNILAC

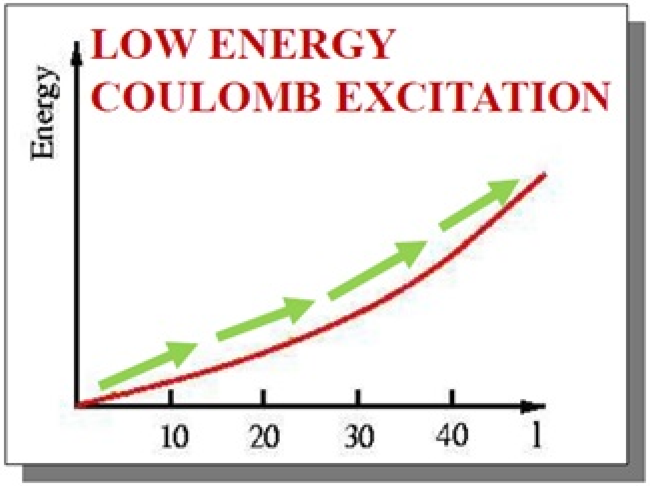

First Coulomb excitation experiment at UNILAC 1980

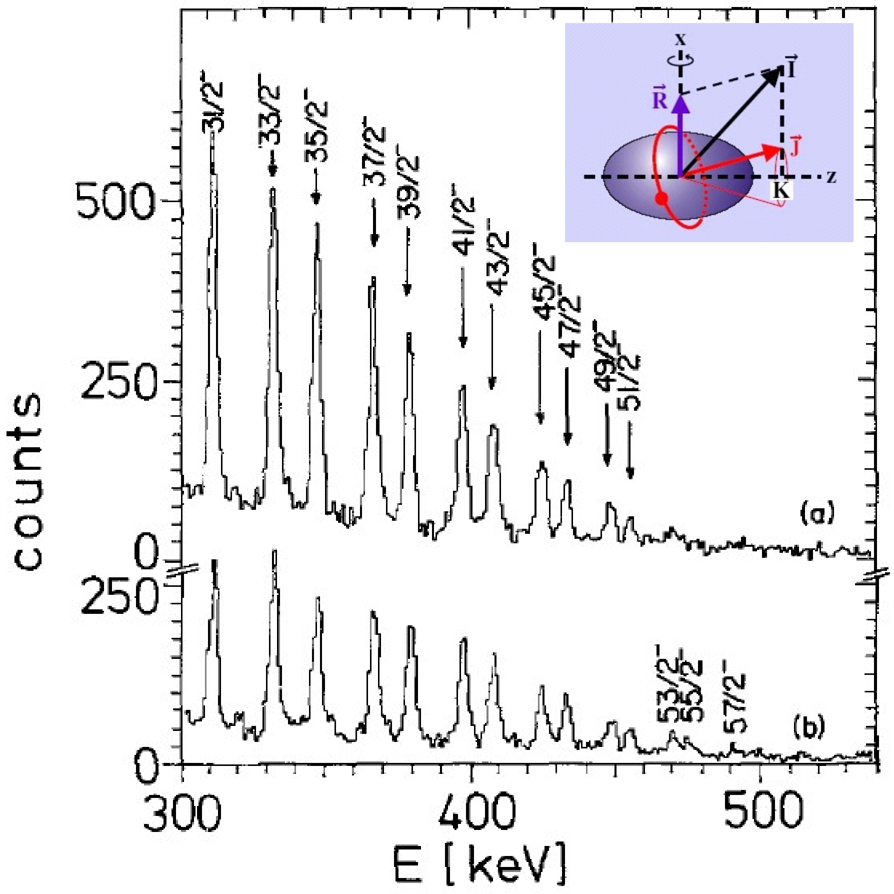

Doppler-corrected γ-ray spectrum for ^{235}U

^{208}Pb (5.3MeV/u) ⟶ ^{235}U

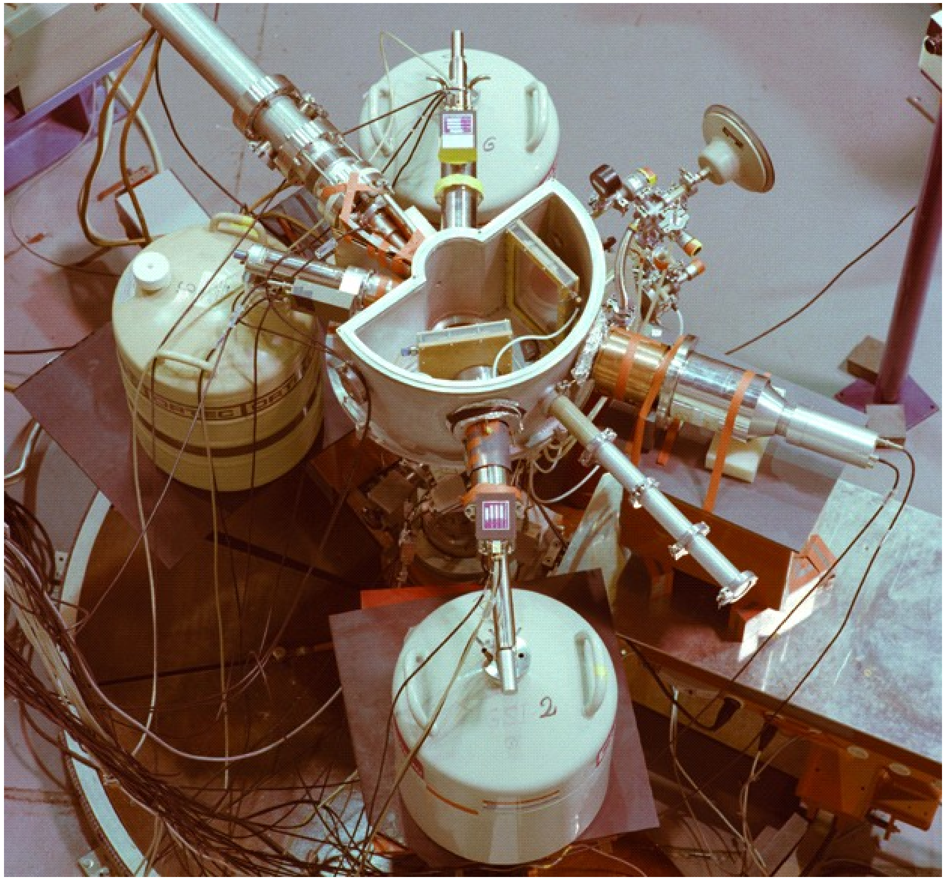

$i_{13/2}$ proton and $j_{15/2}$ neutron alignment in ^{235}U and ^{237}Np

Count rate estimate for UNILAC experiments

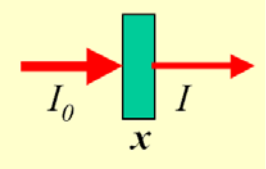

Reaction rate [s^{-1}] = luminosity · cross section [cm^2]

= projectiles [s^{-1}] · target nuclei [cm^{-2}] · cross section [cm^2]

accelerator current: 1 pnA consists of $6 \cdot 10^9$ projectiles [s^{-1}]

target thickness: 1 mg/cm^2 $\quad \dfrac{6 \cdot 10^{23} \cdot 10^{-3} [g/cm^2]}{A_{target} [g]} = target\ nuclei\ [cm^{-2}]$

A_{target}	target nuclei	projectiles	luminosity [s^{-1} cm^{-2}]
200	$3 \cdot 10^{18}$ [cm^{-2}]	$6 \cdot 10^9$ [s^{-1}]	$18 \cdot 10^{27}$ [s^{-1} cm^{-2}]
100	$6 \cdot 10^{18}$ [cm^{-2}]	"	$36 \cdot 10^{27}$ [s^{-1} cm^{-2}]
50	$12 \cdot 10^{18}$ [cm^{-2}]	"	$72 \cdot 10^{27}$ [s^{-1} cm^{-2}]

beam structure:

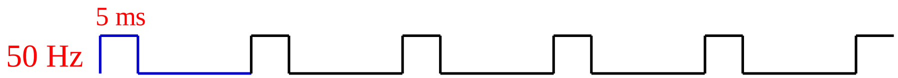

duty factor: 25%

present beam structure:

duty factor: 3%

Coulomb excitation: particle identification

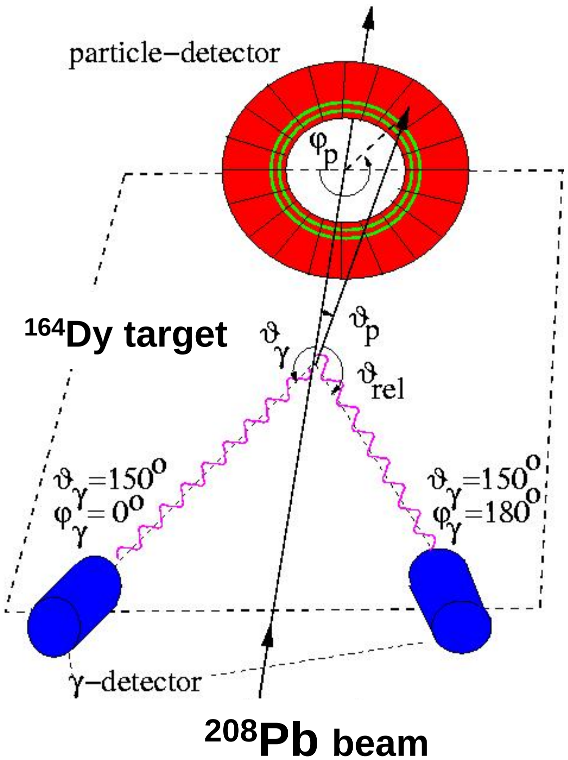

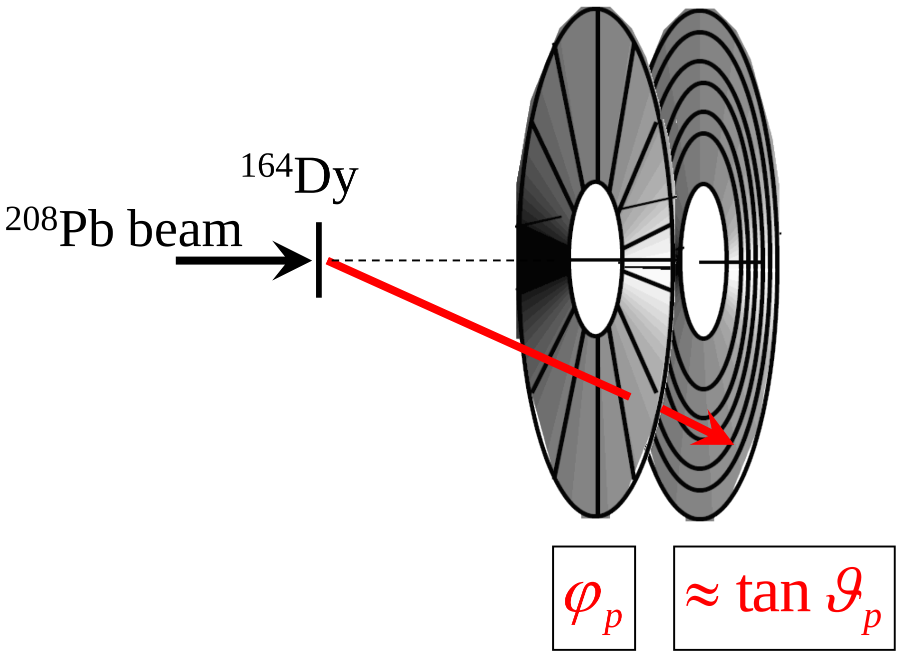

V_0 ~ 500 V
p = 5-10 Torr
gap ~ 3 mm (anode-cathode)

distance target – PPAC: 11 cm

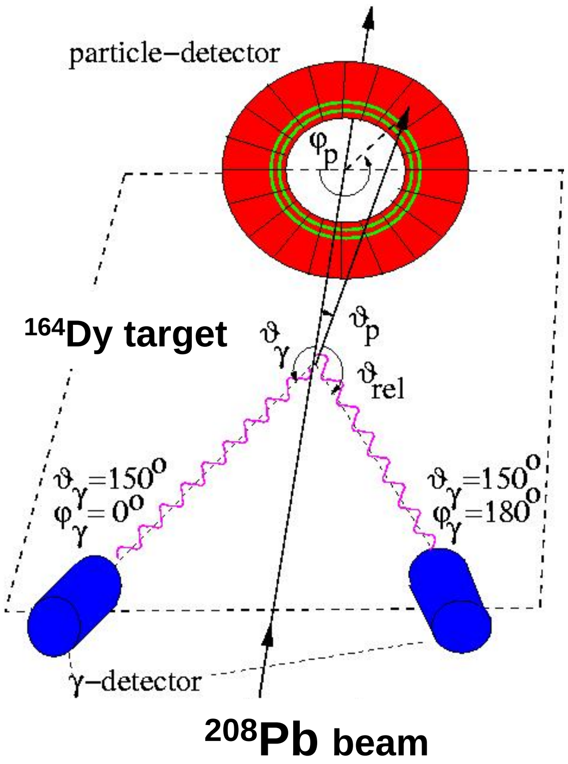

$$max.\,scattering\ angle = arc\ sin\frac{A_2}{A_1}$$

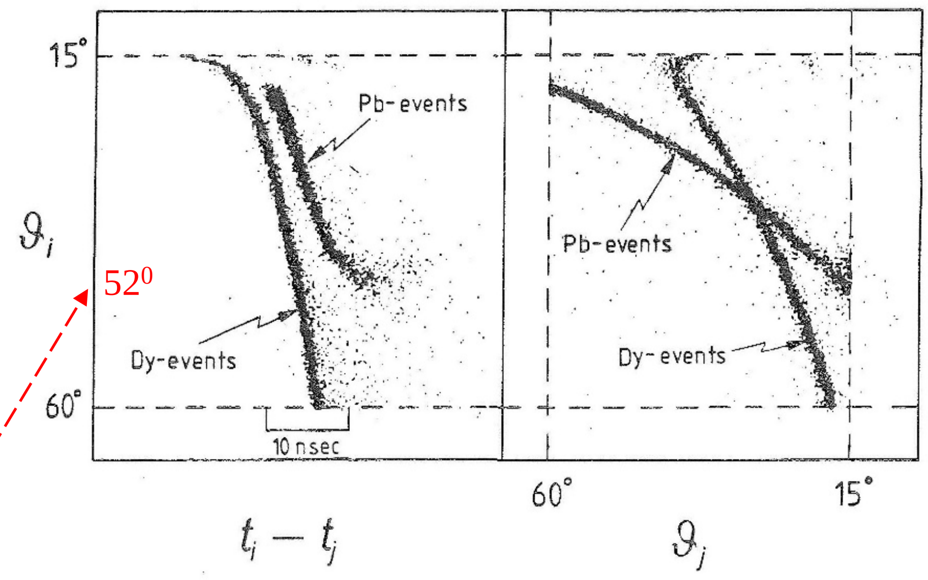

distance target – PPAC: 11 cm

Doppler shift correction ^{208}Pb + ^{164}Dy at 978 MeV

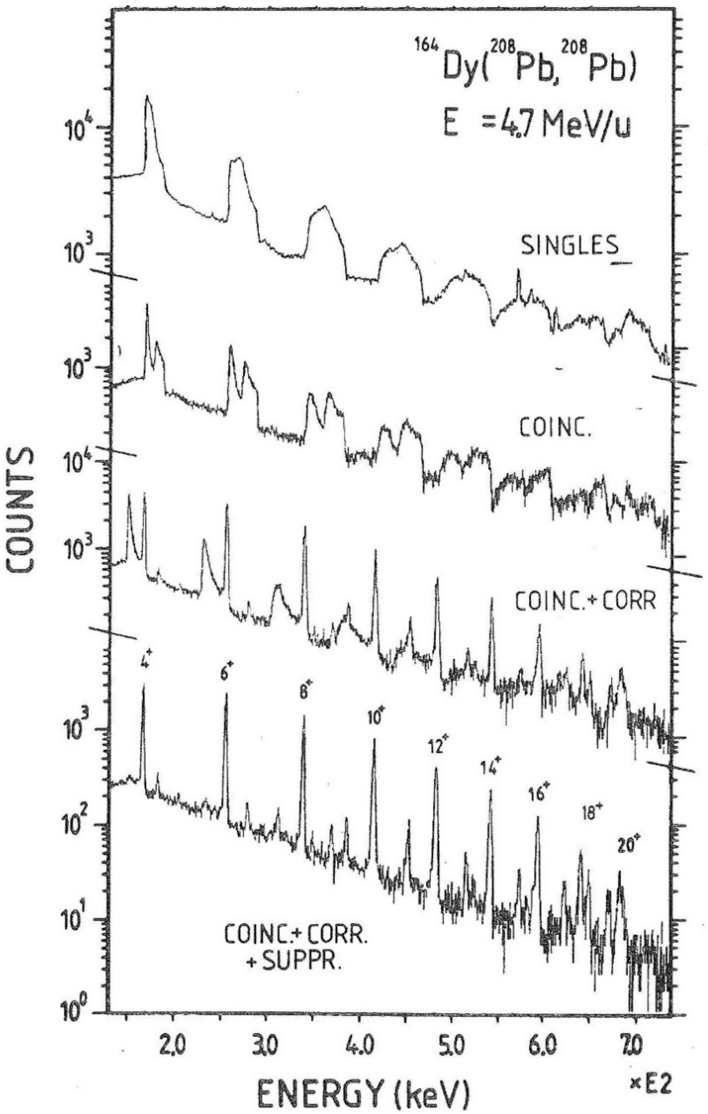

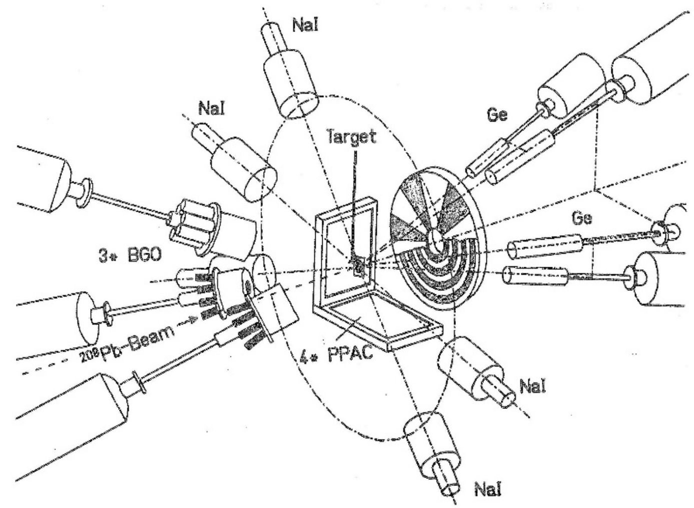

^{164}Dy **target nucleus measured with PPAC** (^{164}Dy **target excitation**)

index 1≡projectile (^{208}Pb) index 2≡target nucleus (^{164}Dy)

$$v_{cm} = 0.04634 \cdot (1 + A_2 / A_1)^{-1} \sqrt{E_{lab} / A_1} \quad (=0.02746)$$

$$v_2 = 2 \cdot v_{cm} \cdot \cos\vartheta_2$$

$$\cos\vartheta_{\gamma 2} = \cos\vartheta_\gamma \cdot \cos\vartheta_2 + \sin\vartheta_\gamma \cdot \sin\vartheta_2 \cdot \cos(\varphi_\gamma - \varphi_2)$$

$$\cos(\varphi_\gamma - \varphi_2) = \cos\varphi_\gamma \cdot \cos\varphi_2 + \sin\varphi_\gamma \cdot \sin\varphi_2$$

$$\frac{E_{\gamma 0}}{E_\gamma} = \frac{1 - v_2 \cdot \cos\vartheta_{\gamma 2}}{\sqrt{1 - v_2^2}}$$

D. Schwalm et al. Nucl.Phys. A192 (1972), 449

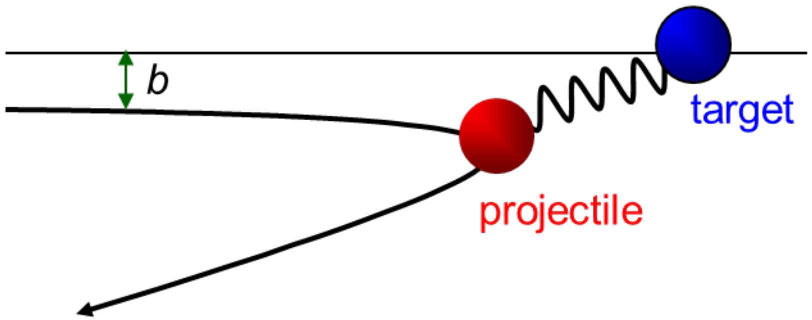

The excitation cross section is a direct measure of the $E\lambda$ matrix elements.

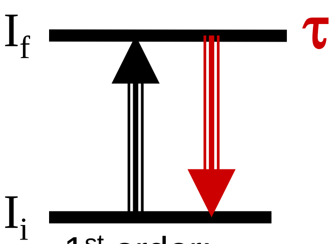

1st order:

$$a^{(1)}_{i\to f} \propto \langle I_f \| \mathbf{M}(E2) \| I_i \rangle$$

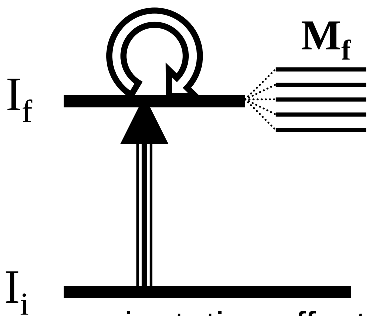

reorientation effect:

$$a^{(2)}_{i\to f} \propto \langle I_f \| \mathbf{M}(E2) \| I_f \rangle \langle I_f \| \mathbf{M}(E2) \| I_i \rangle$$

$$Q_s(2^+) = -\sqrt{\frac{2\pi}{7}\frac{4}{5}} \cdot \langle 2 \| M(E2) \| 2 \rangle$$

$$P^{(2)}_{0\to 2}(\theta,\xi) = P^{(1)}_{0\to 2}(\theta,\xi) \cdot \left[1 + \sqrt{\frac{7}{2\pi}\frac{5}{4}} \cdot \frac{A_p}{Z_p} \cdot \frac{\Delta E}{1 + A_p/A_t} \cdot Q_s(2) \cdot K(\theta,\xi) \right]$$

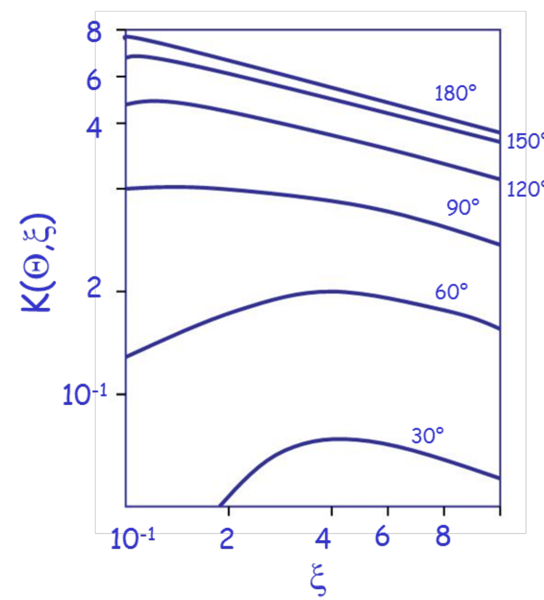

Quadrupole deformation in $^{182,184,186}W$

W176 2.5 h 0+ EC	W177 135 m (1/2-) EC	W178 21.6 d 0+ EC	W179 37.05 m (7/2)- * EC	W180 0+ * 0.13	W181 121.2 d 9/2+ EC	W182 0+ 26.3	W183 1.1E+17 y 1/2- * 14.3	W184 3E+17 y 0+ 30.67	W185 75.1 d 3/2- * β-	W186 0+ 28.6	W187 23.72 h 3/2- β-	W188 69.4 d 0+ β-	W189 11.5 m (3/2-) β-	W190 30.0 m 0+ β-
Ta175 10.5 h 7/2+ EC	Ta176 8.09 h (1)- * EC	Ta177 56.56 h 7/2+ EC	Ta178 9.31 m 1+ * EC	Ta179 1.82 y 7/2+ * EC	Ta180 8.152 h 1+ EC,β- * 0.012	Ta181 7/2+ 99.988	Ta182 114.43 d 3- * β-	Ta183 5.1 d 7/2+ β-	Ta184 8.7 h (5-) β-	Ta185 49.4 m (7/2+) β-	Ta186 10.5 m 2,3 β-	Ta187	Ta188	116
Hf174 2.0E15 y 0+ α 0.162	Hf175 70 d 5/2- EC	Hf176 0+ 5.206	Hf177 7/2- * 18.606	Hf178 0+ * 27.297	Hf179 9/2+ * 13.629	Hf180 0+ * 35.100	Hf181 42.39 d 1/2- β-	Hf182 9E6 y 0+ * β-	Hf183 1.067 h (3/2-) β-	Hf184 4.12 h 0+ β-	Hf185 3.5 m β-	Hf186 0+		

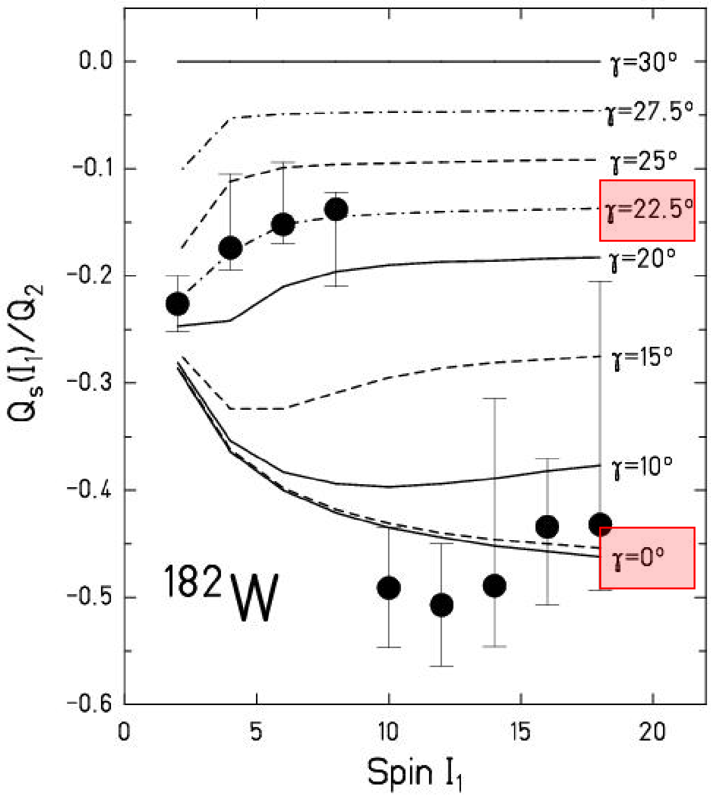

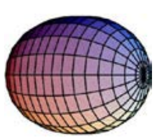

prolate

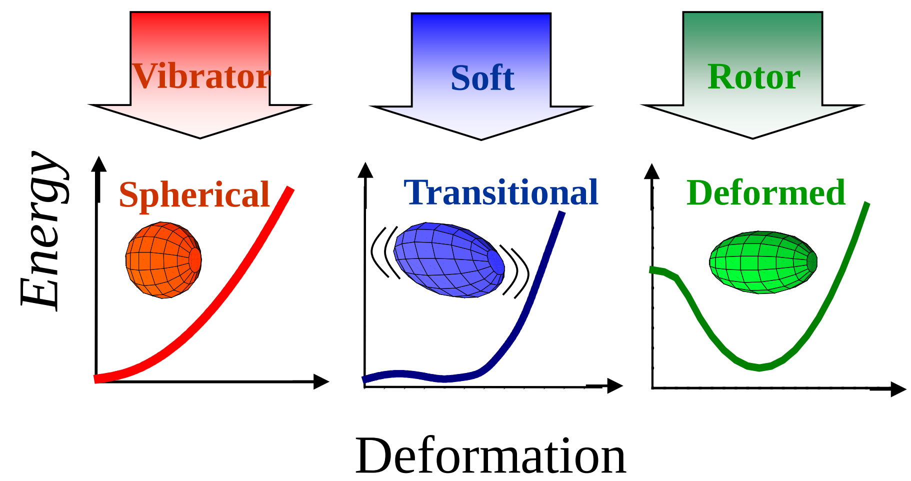

R. Kulessa et al., Phys. Lett. B218 (1989), 421

Alignment of $i_{13/2}$ protons in ^{242,244}Pu

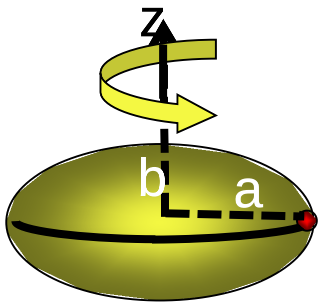

$$E_I = \frac{\hbar^2}{2\Im} I(I+1)$$

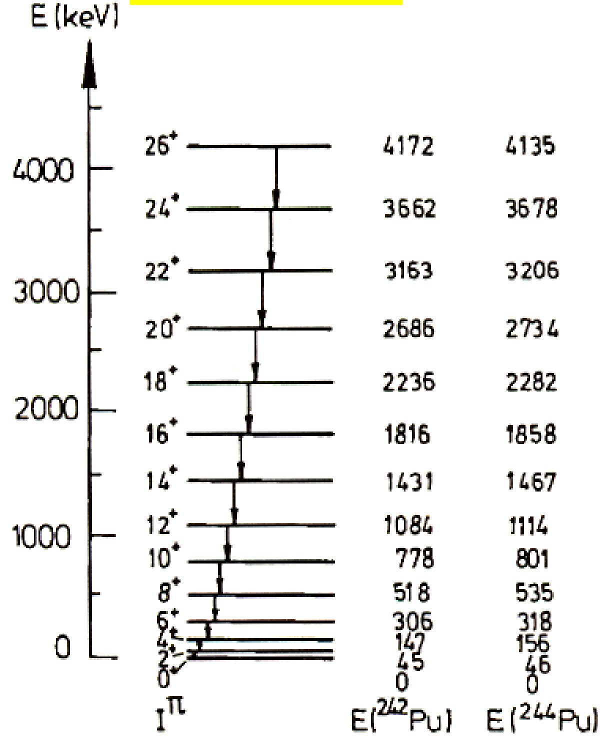

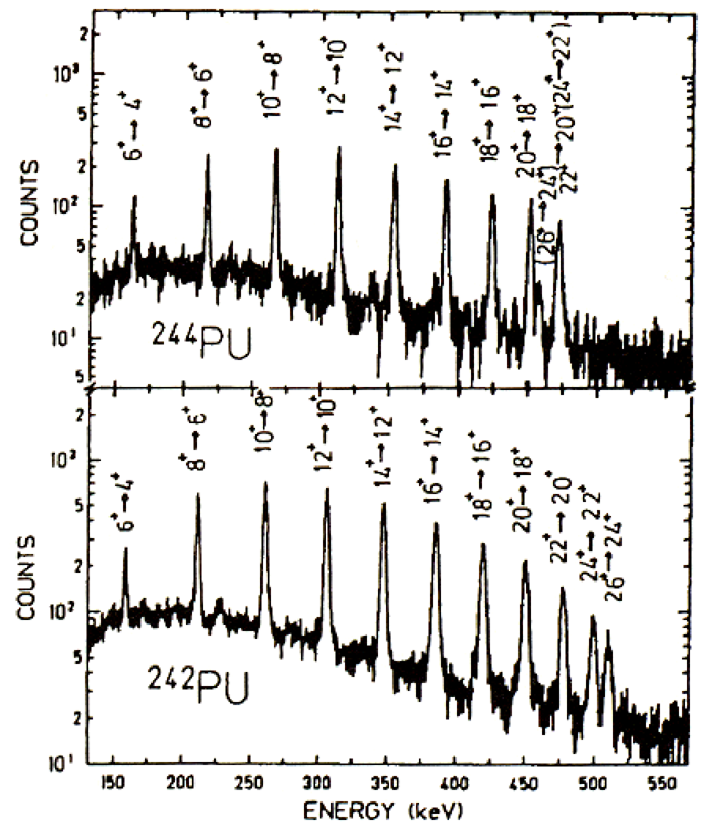

$$E_\gamma = E_I - E_{I-2} = \frac{\hbar^2}{2\Im}(4I-2)$$

$$\Im = \frac{2}{5} A \cdot M \cdot R_0^2 \cdot \beta^2$$

$$B(E2; I \to I-2) = \frac{15}{32\pi} \frac{I(I+1)}{(2I-1)(2I+1)} \cdot Q_2$$

$$Q_2 = \frac{3ZR_0^2}{\sqrt{5\pi}} \cdot \beta$$

- analysis with GOSIA code

W. Spreng et al., Phys. Rev. Lett. 51 (1983), 1522

Coulomb excitation of ^{114}Sn projectile excitation

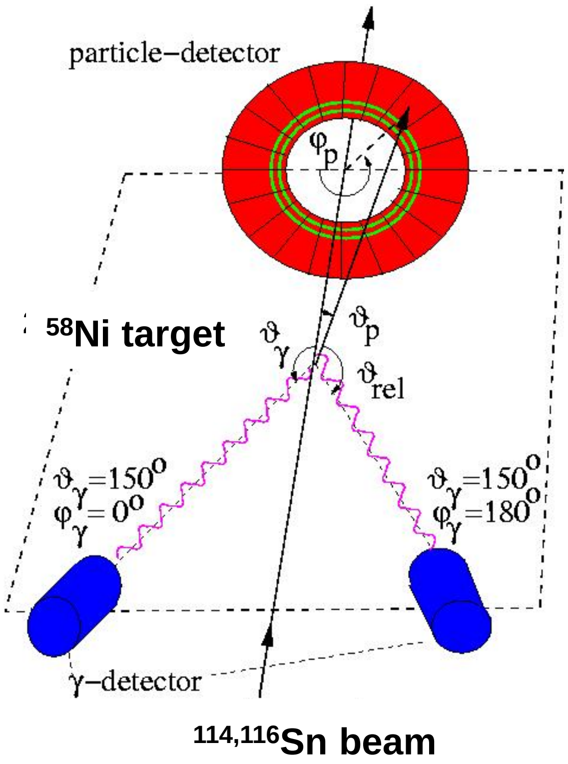

^{114,116}Sn→^{58}Ni at 3.6MeV/u

E_x=1300, 1294 MeV
B(E2)↑=0.25(5), 0.209(5)e^2b^2

γ-efficiency = 0.005
accelerator duty factor=10%

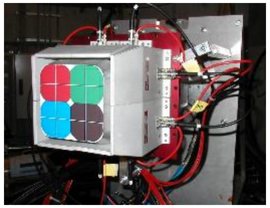

beam intensity = 1pnA
target thickness = 1mg/cm^2

pγ-rate (Sn) = 1/s

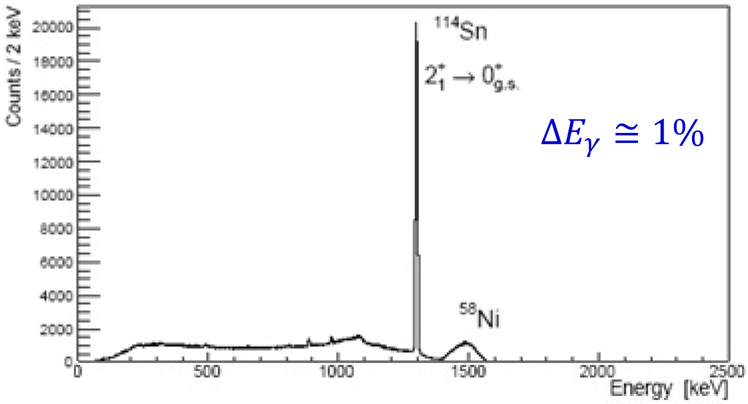

natural abundance of ^{114}Sn: 0.65%

P. Doornenbal, A.Jhingan, R.Kumar, et al., Phys.Rev C 78 (2008) 031303

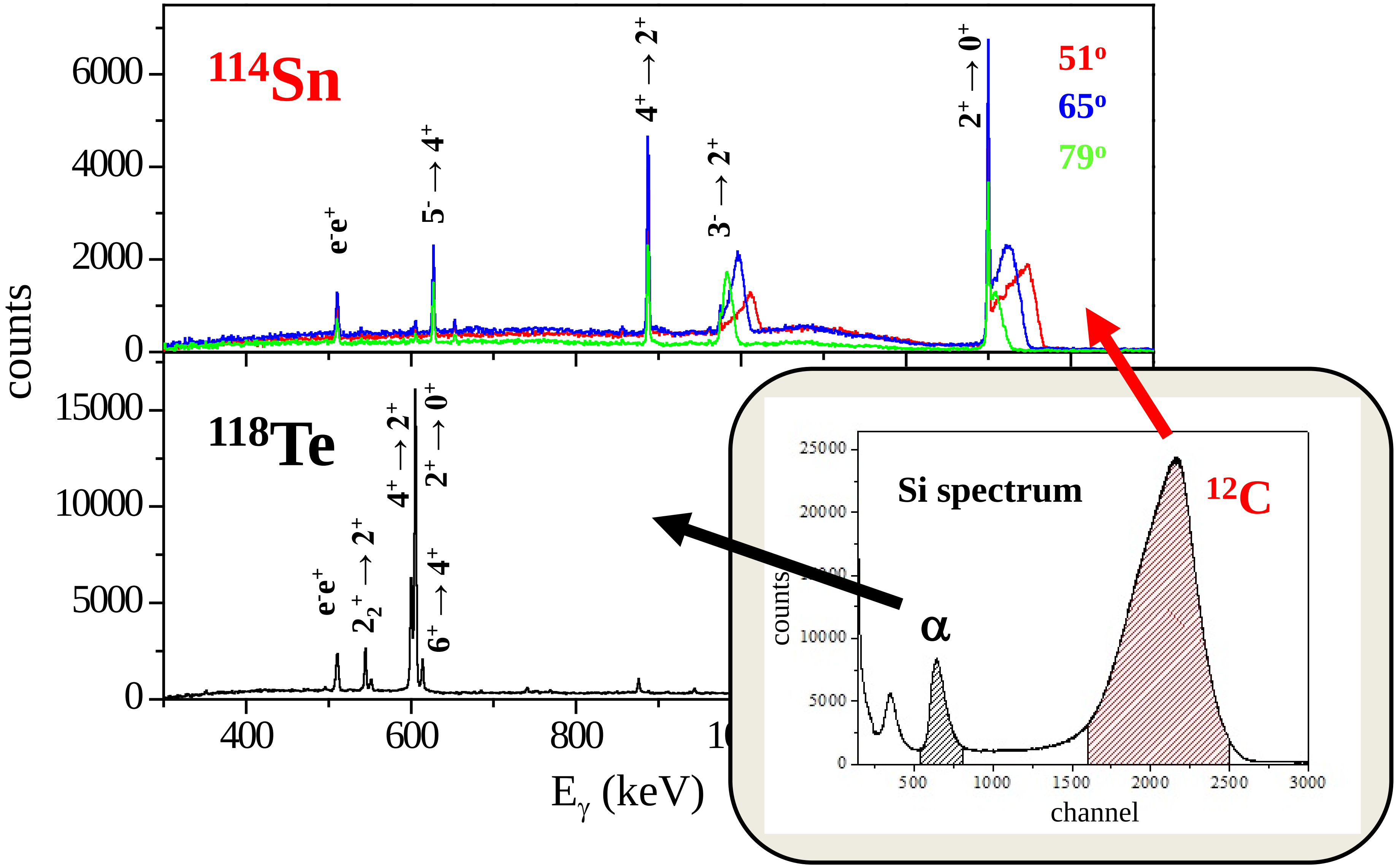
counts
^{114}Sn
6000
4000
2000
0
e⁻e⁺
5⁻ → 4⁺
4⁺ → 2⁺
3⁻ → 2⁺
2⁺ → 0⁺
51°
65°
79°
^{118}Te
15000
10000
5000
0
e⁻e⁺
2_2^+ → 2⁺
4⁺ → 2⁺
2⁺ → 0⁺
6⁺ → 4⁺
400
600
800
E$_\gamma$ (keV)
Si spectrum
^{12}C
α
counts
25000
20000
10000
5000
0
500
1000
1500
2000
2500
3000
channel

α-clustering in ^{12}C

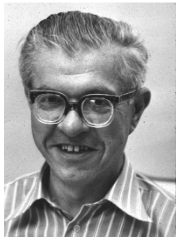

Fred Hoyle 1953

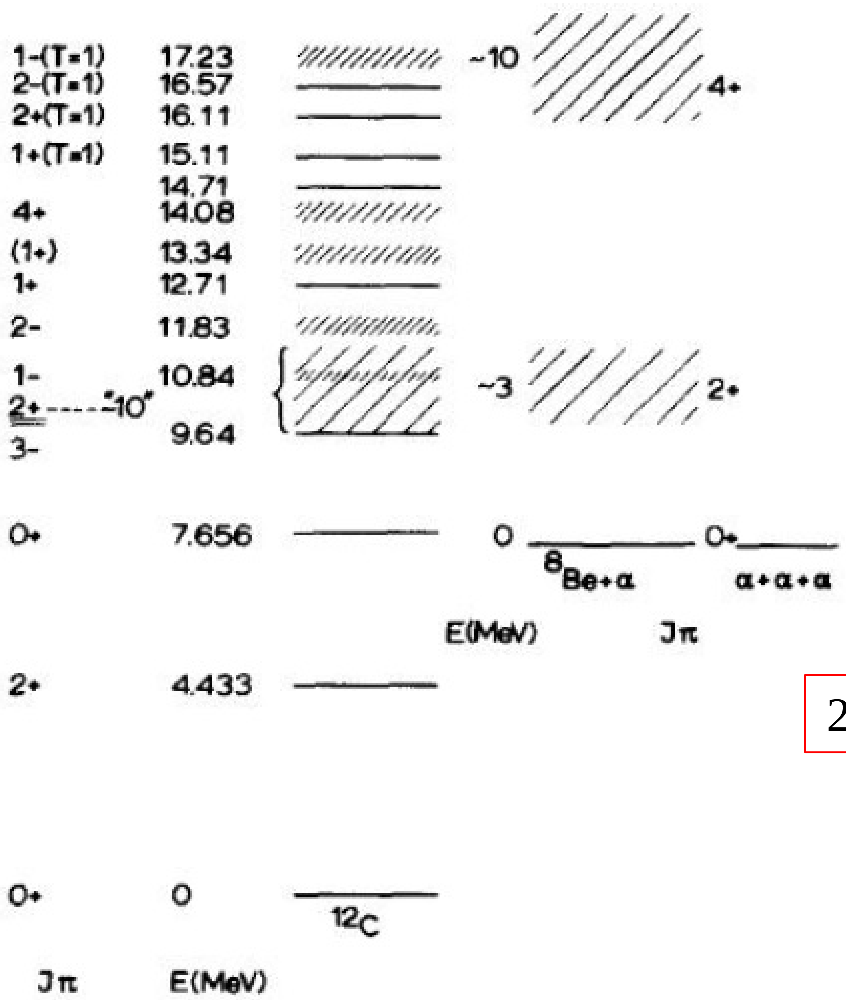

Haruhiko Morinaga
1956

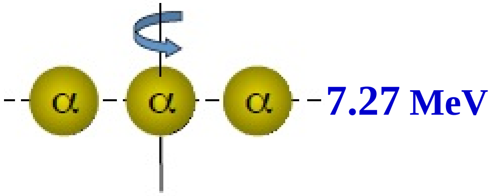

2.4 MeV per bound

α-transfer experiment

$^{112,114,116}Sn + {}^{12}C \;<\; {}^{112,114,116}Sn^{*}$ / ${}^{116,118,120}Te^{*}$

$$456\ MeV \rightarrow\ \theta_{1/4}^{cm} = 115.5^0$$

$$\varsigma_{1/4}^{lab}({}^{12}_{6}C) = 32.2^0$$

4 Euroball Cluster at ±65°

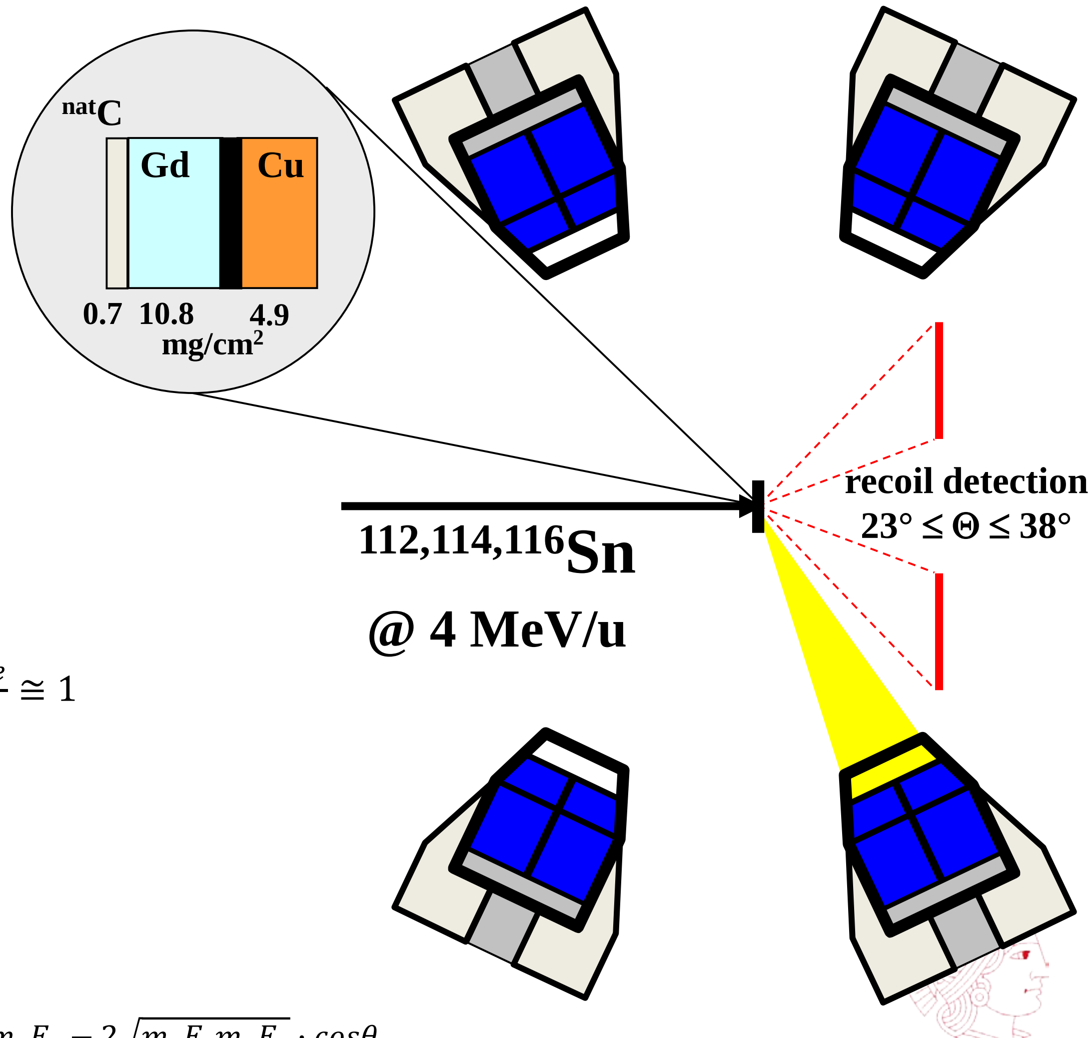

delayed breakup

$^{8}Be\ 0^{+}\ \tau \sim 10^{-15}\ s$

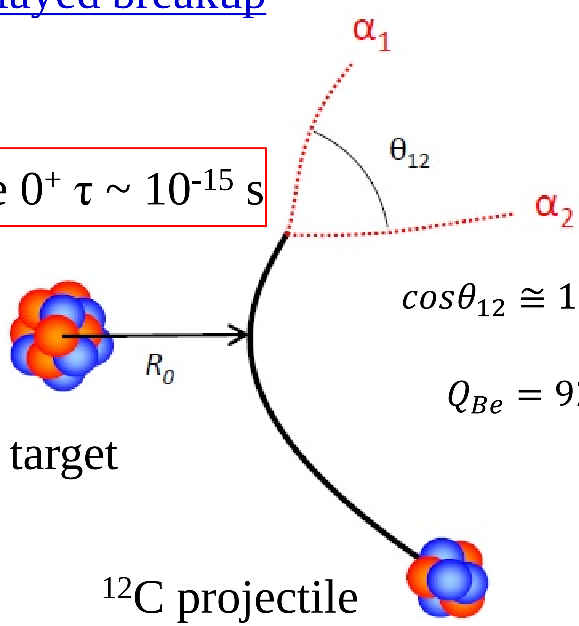

$$cos\theta_{12} \cong 1 - \frac{Q_{Be}}{E_1} \cong 1$$

$$Q_{Be} = 92\ keV$$

$$E_{rel} = \frac{m_2E_1 + m_1E_2 - 2\sqrt{m_1E_1m_2E_2} \cdot cos\theta_{12}}{m_1 + m_2}$$

Transient magnetic fields g-factor measurement

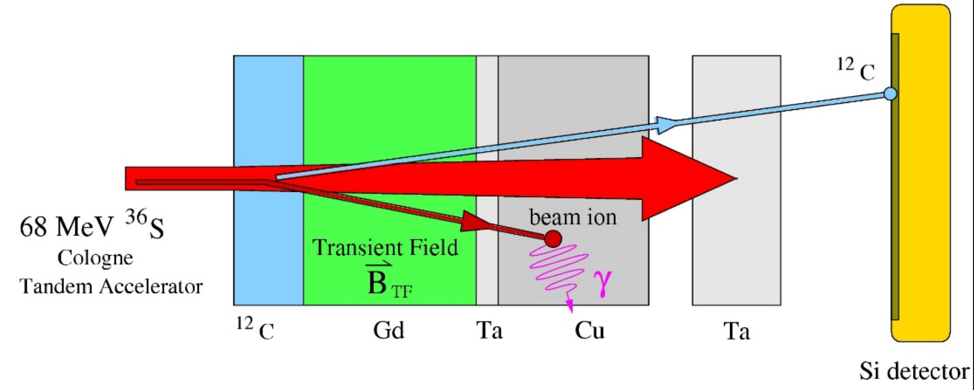

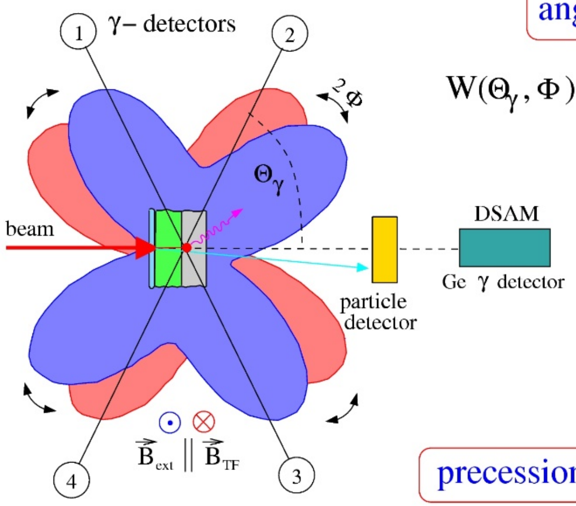

angular correlation

$$W(\Theta_\gamma, \Phi) = \sum_{k=0,2,4,..}^{k_{max}} Q_k \cdot A_k \cdot P_k\,(\cos(\Theta_\gamma \pm \Phi))$$

double ratio:

$$DR(1/4) = \frac{N1\uparrow}{N1\downarrow} \div \frac{N4\uparrow}{N4\downarrow}$$

precession angle

$$\Phi = \frac{\sqrt{DR} - 1}{\sqrt{DR} + 1} \Big/ \frac{1}{W} \cdot \left.\frac{dW}{d\Theta}\right|_{\Theta_\gamma} = g\,\frac{\mu_N}{\hbar} \int_{t_{in}}^{t_{out}} B_{TF}(v_{ion})\, e^{-\frac{t}{\tau}}\, dt$$

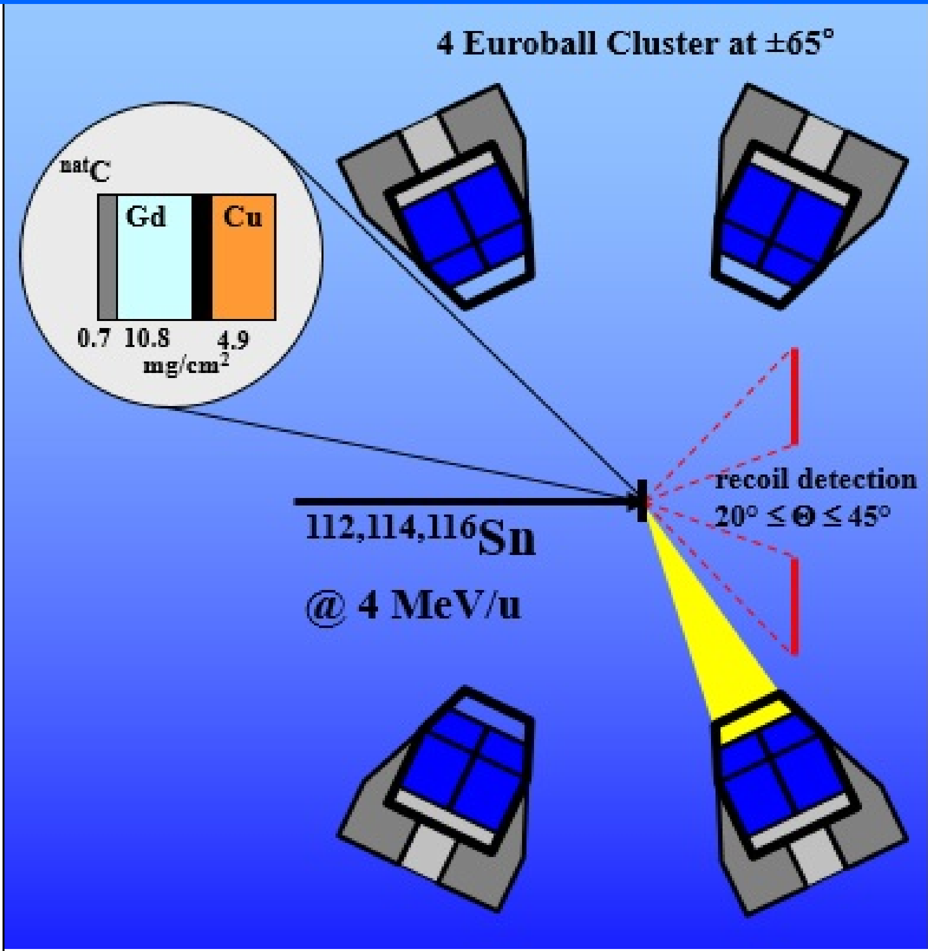

Space inversion invariance: octupole deformed nucleus ^{226}Ra

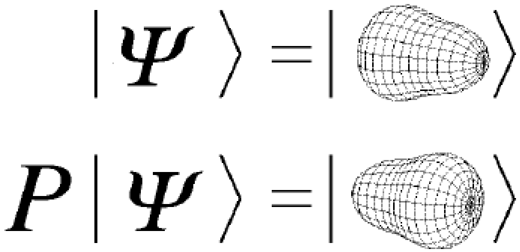

$$P|\Psi\rangle \neq |\Psi\rangle$$

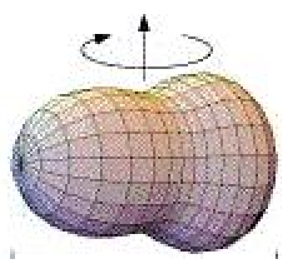

rotation

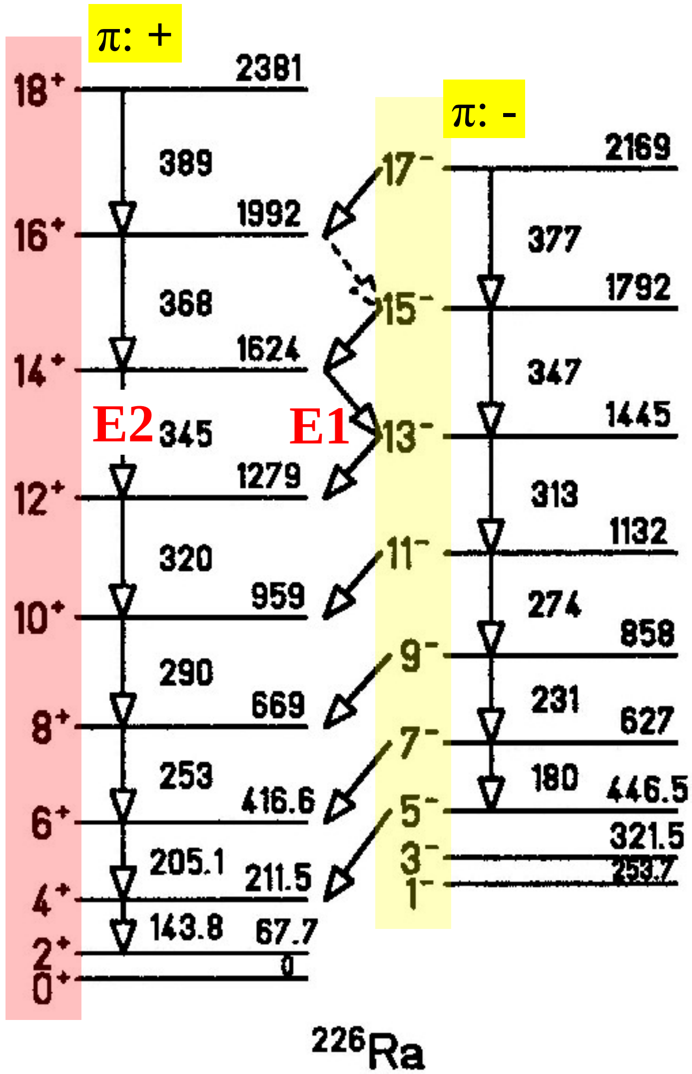

H.J.Wollersheim, C. Fleischmann et al., Nucl. Phys. A556 (1993), 261

Coulomb excitation of ^{226}Ra

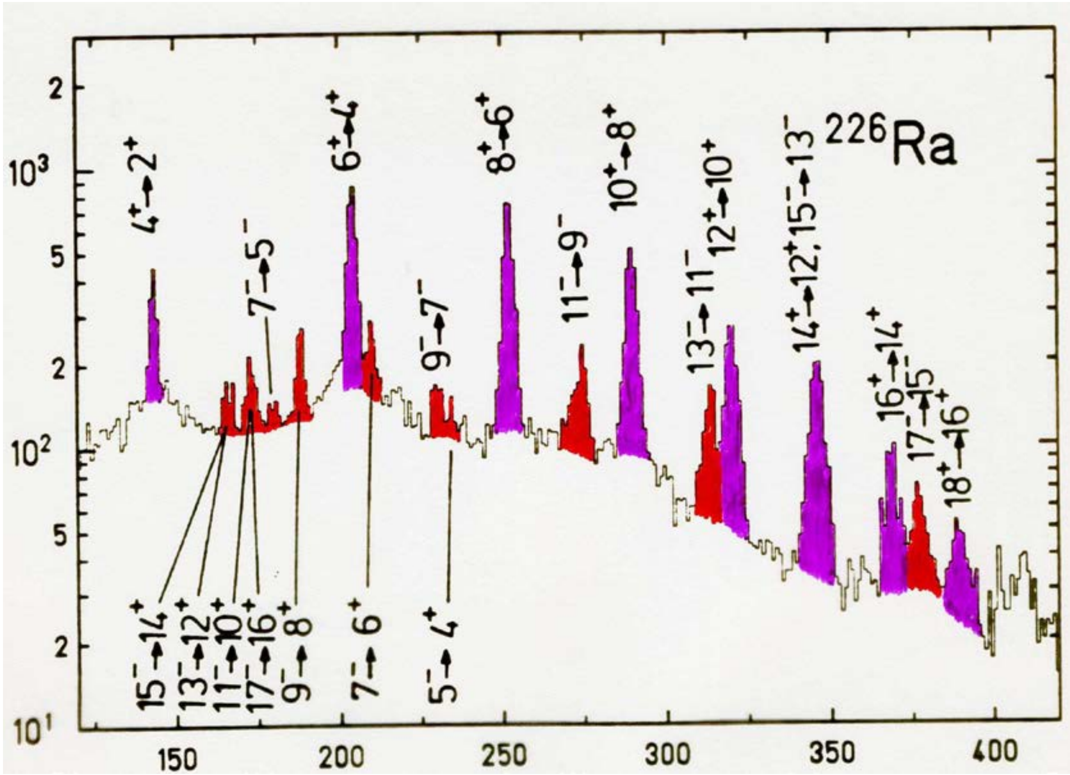

counts

energy [keV]

^{208}Pb → ^{226}Ra

E_{lab} = 4.7 AMeV

$15^0 \leq \theta_{lab} \leq 45^0$

$0^0 \leq \varphi_{lab} \leq 360^0$

^{226}Ra target broken after 8 hours

H.J.Wollersheim, C. Fleischmann et al., Nucl. Phys. A556 (1993), 261

Coulomb excitation of ^{226}Ra 1992

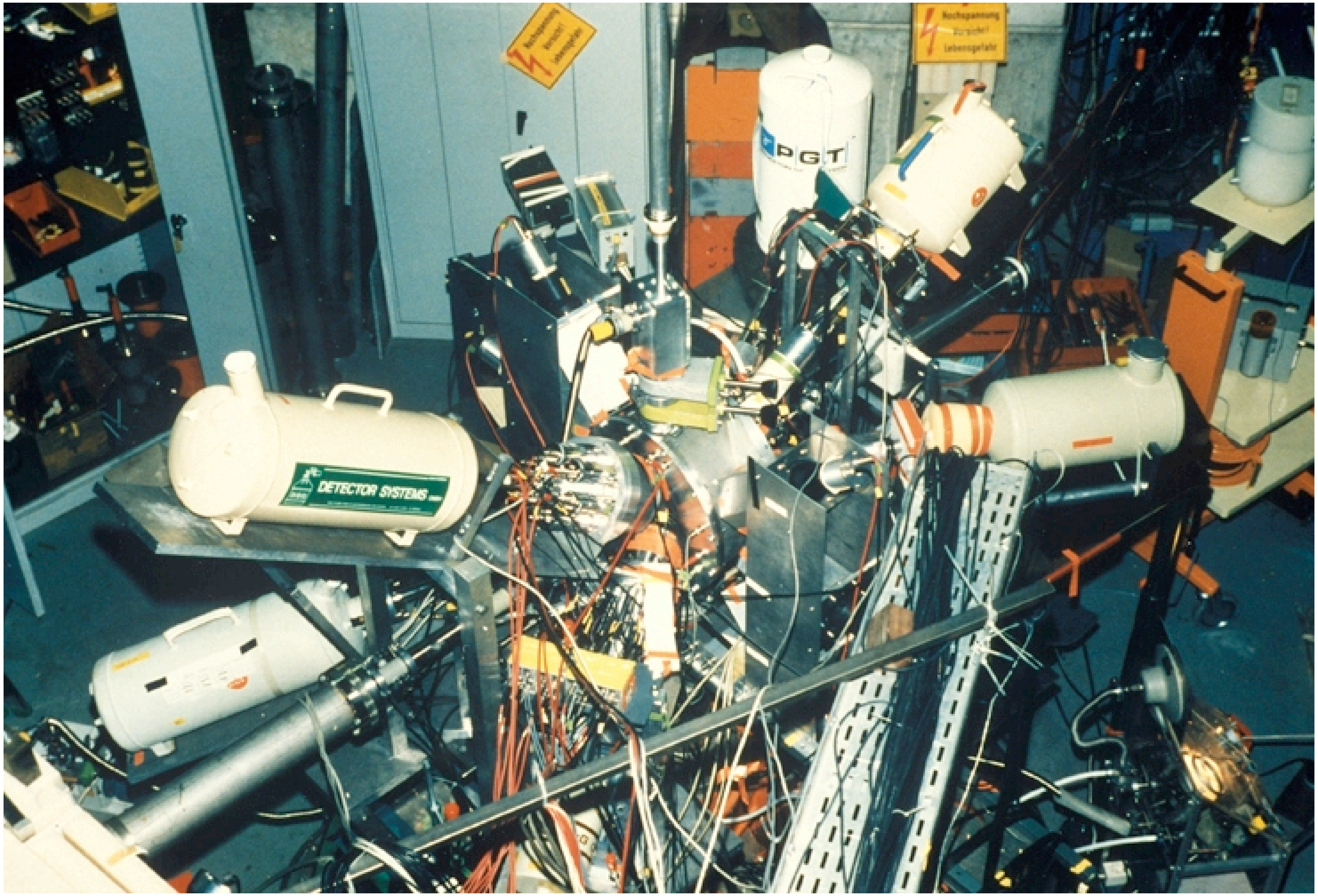

Conversion electrons

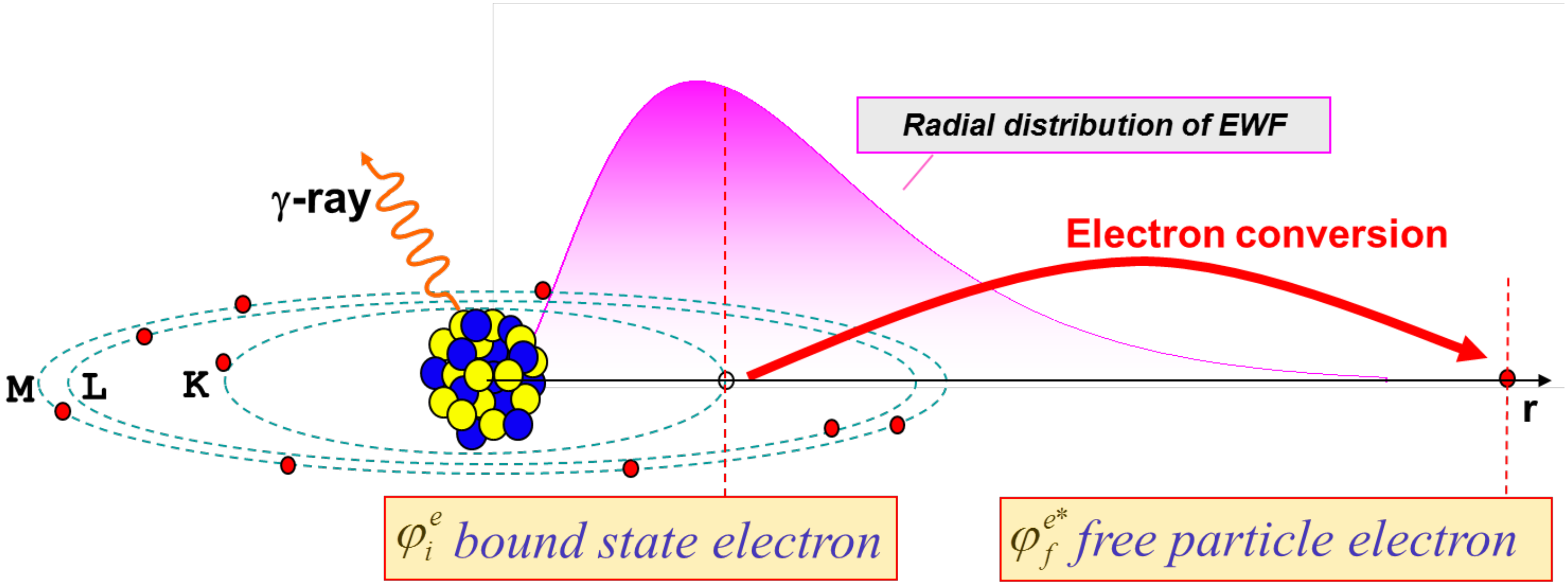

❖ For an electromagnetic transition internal conversion can occur instead of emission of gamma radiation. In this case the transition energy $Q = E_\gamma$ will be transferred to an electron of the atomic shell.

$$T_e = E_\gamma - B_e$$

T_e: kinetic energy of the electron
B_e: binding energy of the electron

internal conversion is important for:
- heavy nuclei ~ Z^3
- high multipolarities Eℓ or Mℓ
- small transition energies

$$\alpha_k(El) \propto Z^3 \left(\frac{L}{L+1}\right)\left(\frac{2m_e c^2}{E}\right)^{L+5/2}$$

Electron spectroscopy with Mini-Orange devices

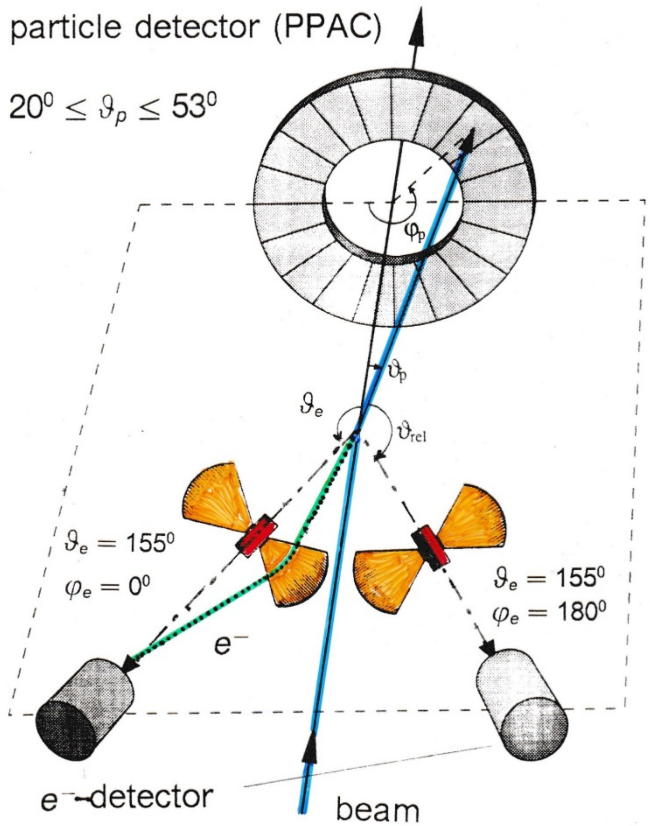

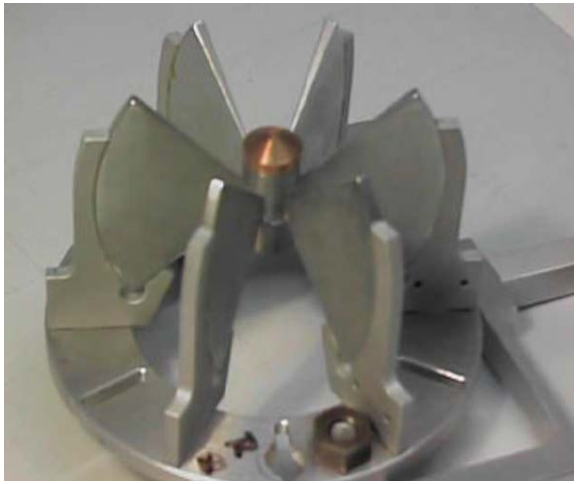

$\Delta\vartheta_e = 20^0$
target – Mini-Orange: 19 cm
Mini-Orange – Si detector: 6 cm

Doppler correction for projectile excitation:

$$T_e^* = \gamma \cdot T_e \cdot \left\{1 - \beta_1 \cdot \sqrt{1 + 2m_e\, c^2/T_e} \cdot cos\theta_{e1}\right\} + m_e c^2 \cdot (\gamma - 1)$$

$$cos\theta_{e1} = cos\vartheta_1 cos\vartheta_e + sin\vartheta_1 sin\vartheta_e cos(\varphi_e - \varphi_1)$$

Doppler-corrected e⁻- and γ-ray spectra

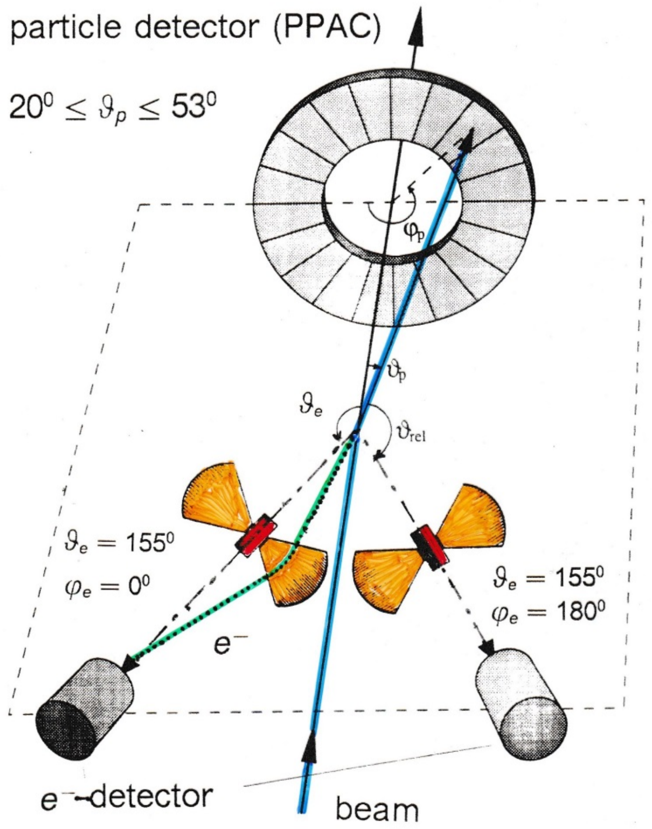

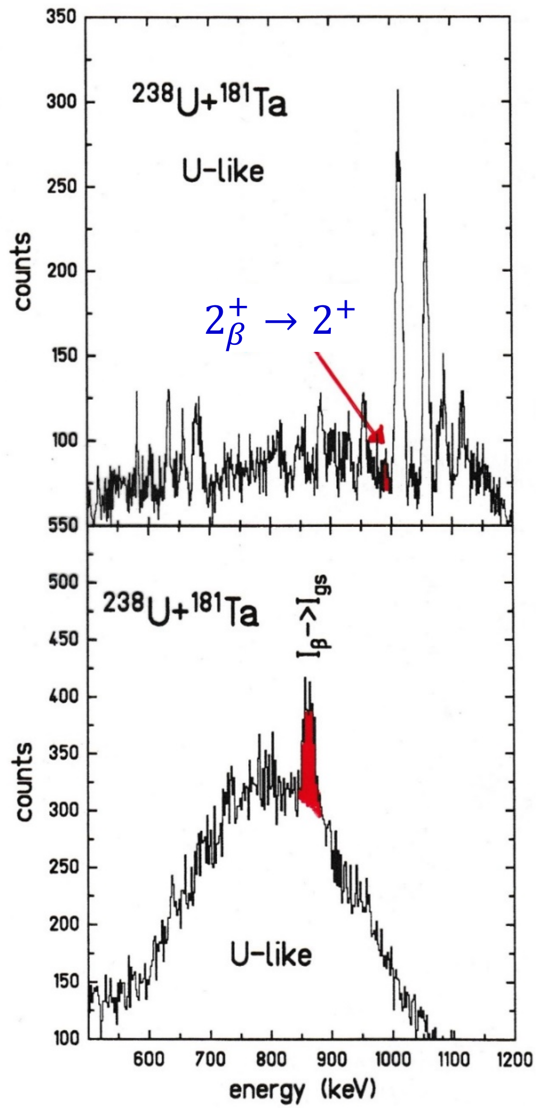

γ-ray spectrum

e⁻ spectrum

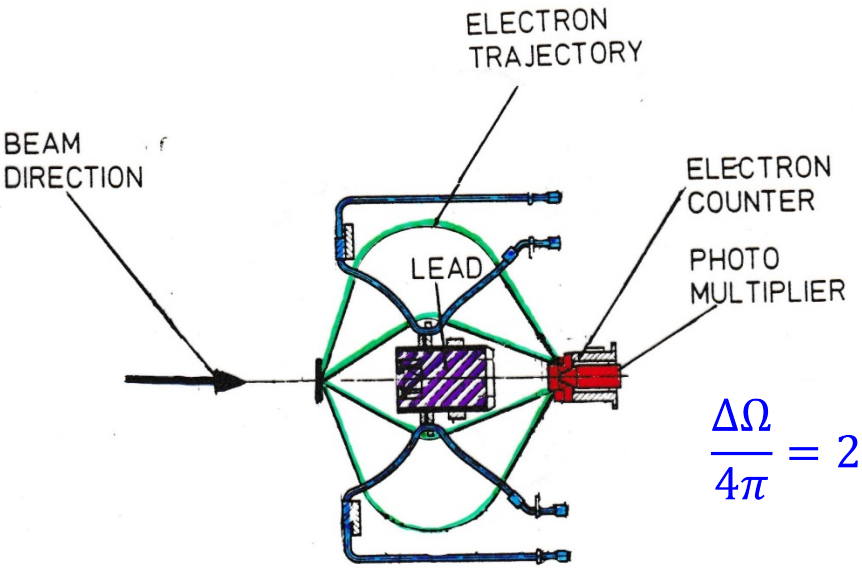

$$\frac{\Delta\Omega}{4\pi} = 26\%$$

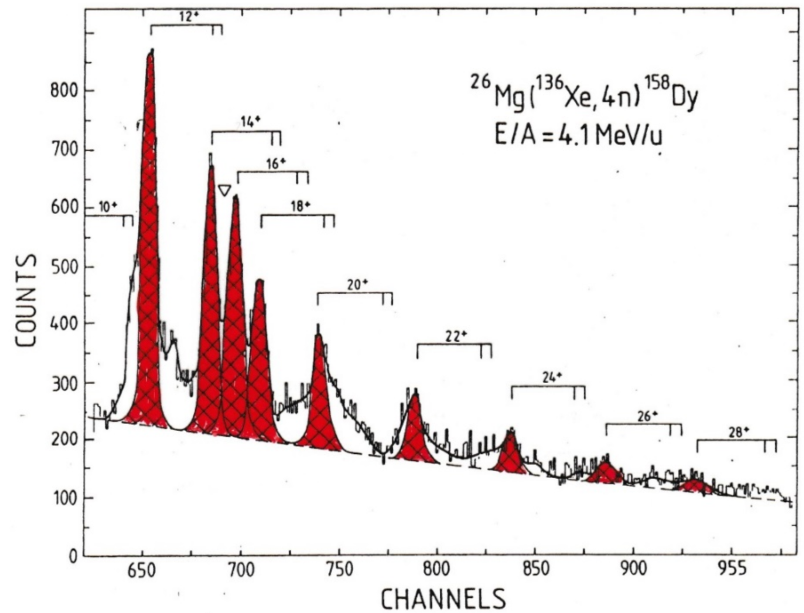

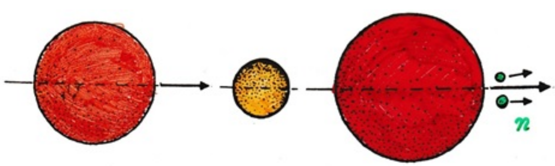

$^{136}Xe + ^{26}Mg \rightarrow ^{158}Dy$

$$\vartheta_c = 0^0$$

$$\beta_c = \beta_{cm} = 0.079$$

		$(\frac{\Delta p}{p})_e / \%$
resolution of the spectrometer including Doppler correction as calculated for a point source		0.4
scattering in the target	(i)	0.004
beam optics	(ii)	0.11
evaporation of neutrons	(iii)	0.09
energy loss in the target	(iv)	0.31
energy straggling of the projectiles	(v)	0.006
quadratic sum		0.53
experimental resolution		0.56

%

L. Handschug et al.; NIM 161 (1979) 117

Nuclear structure of ^{178}Hf

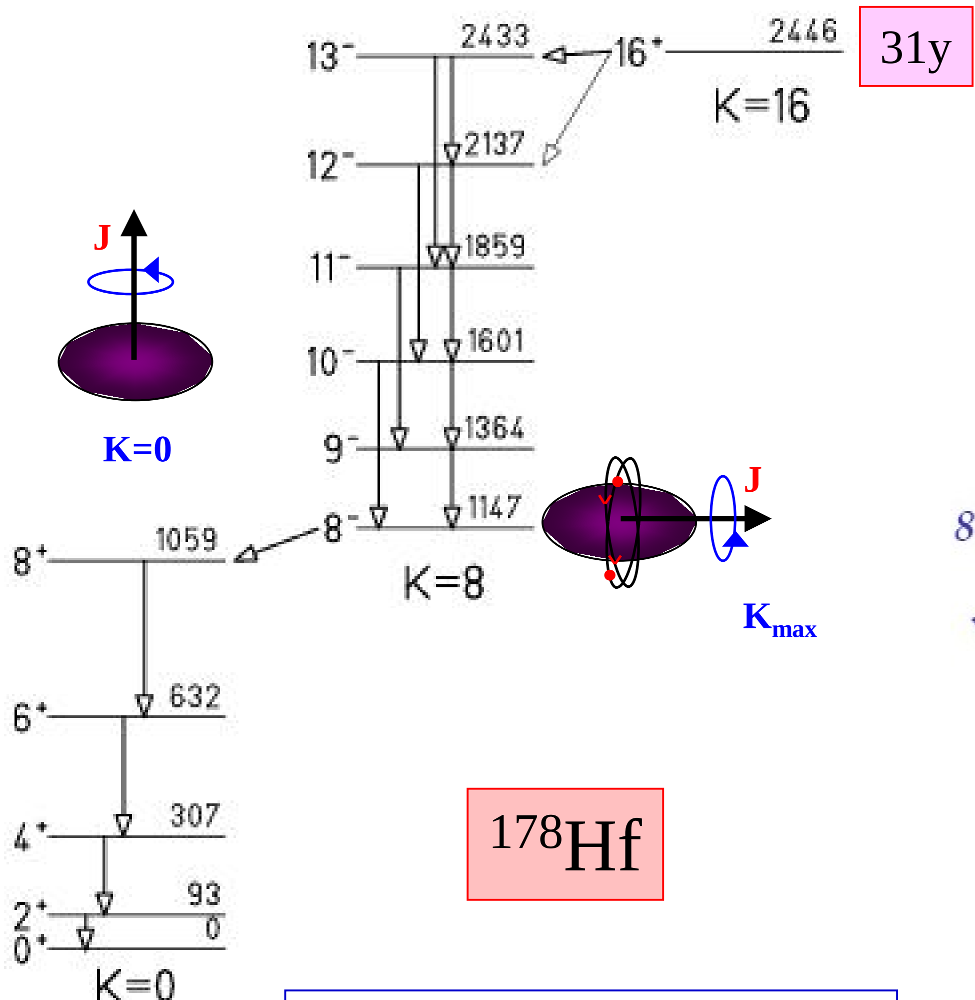

^{178}Hf

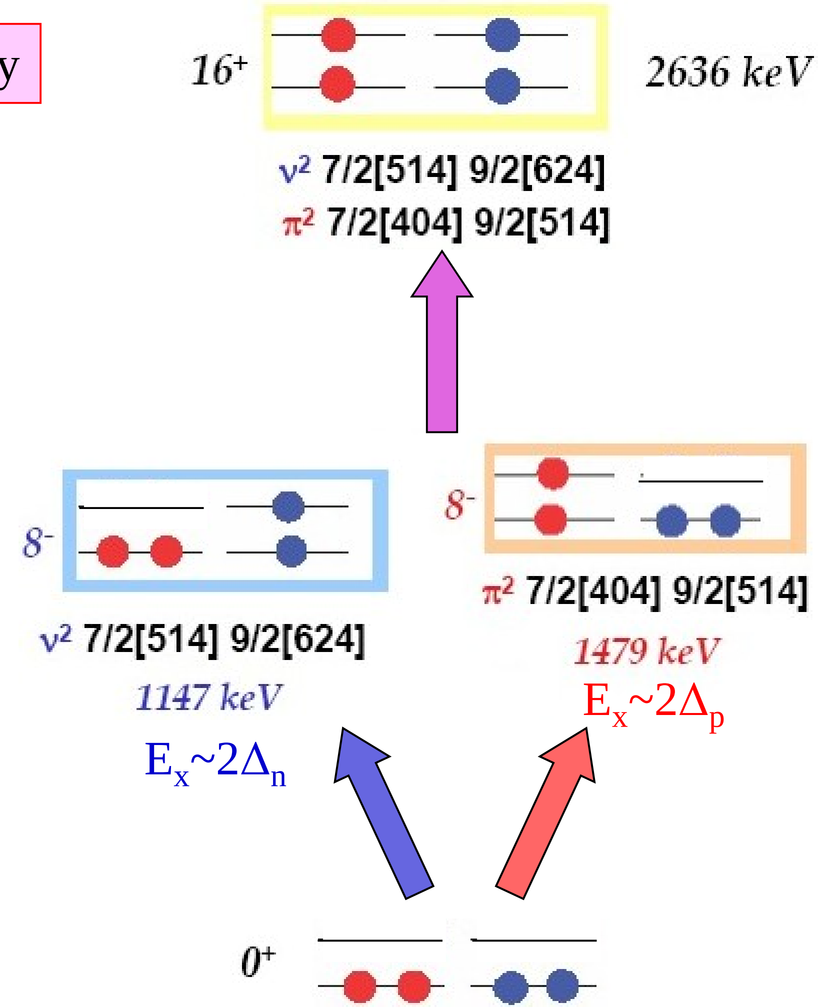

high-K orbitals near the Fermi surface

$\nu: f_{7/2}\, i_{13/2} \quad \pi: h_{11/2}\, g_{7/2}$

Coulomb excitation of the K = 8⁻ isomer in ^{178}Hf

- ^{178}Hf + ^{130}Te at 560, 590, 620 MeV

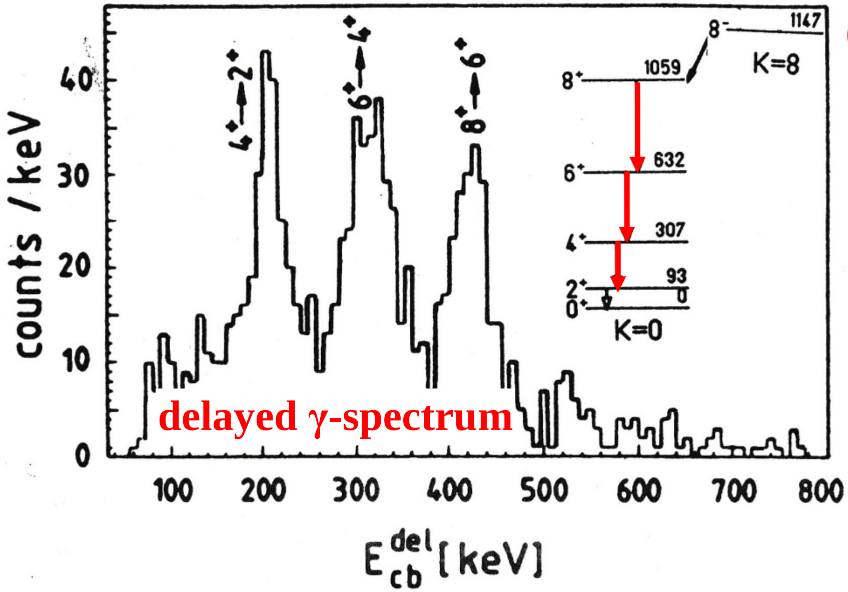

4 s → M_{30} $(E3)$

Delayed γ-ray spectrum of the Crystal Ball with $850 keV \le E_{sum}^{del} \le 1100 keV$ and $3 \le N_{det} \le 6$. In addition at least one of the delayed γ-rays must have been detected in one of the Ge-detectors.

Darmstadt Heidelberg
Crystal Ball

ΔE_γ = 90 keV

H. Xie et al.; Phys. Rev. C48 (1993), 2517

Darmstadt-Heidelberg Crystal Ball and EUROBALL-3 demonstrator 1993

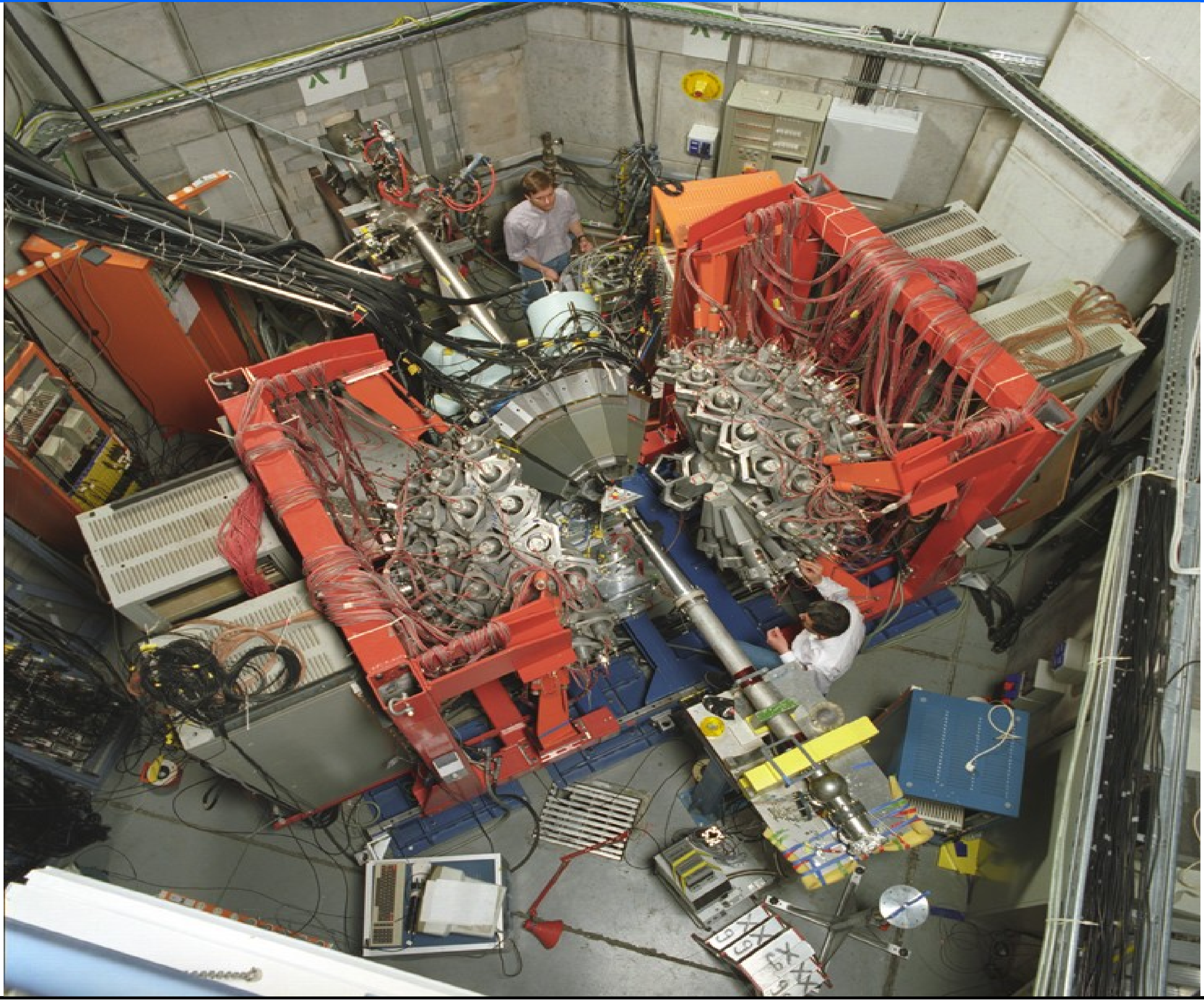

Doppler shift attenuation method

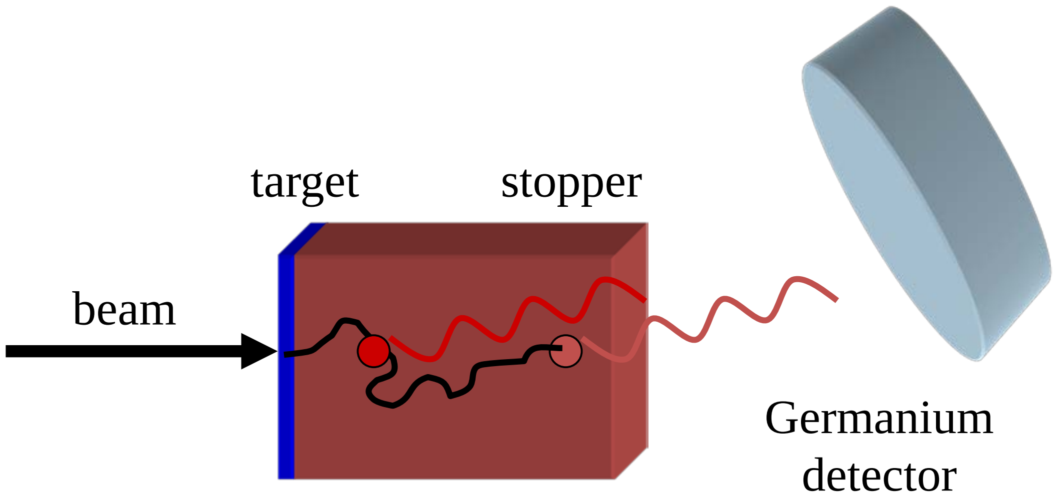

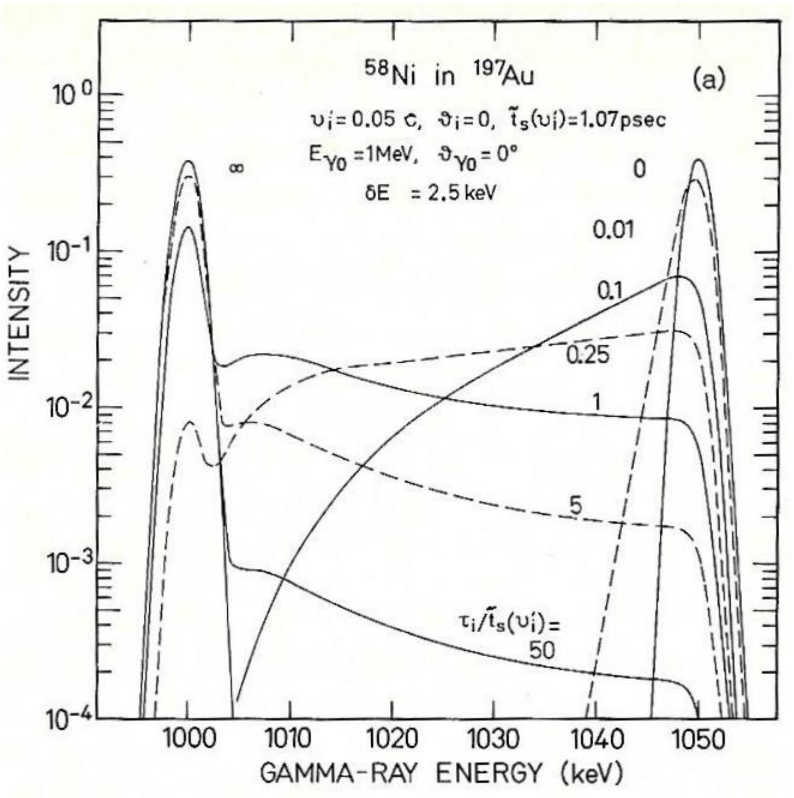

Spectroscopy of binary and ternary fission fragments

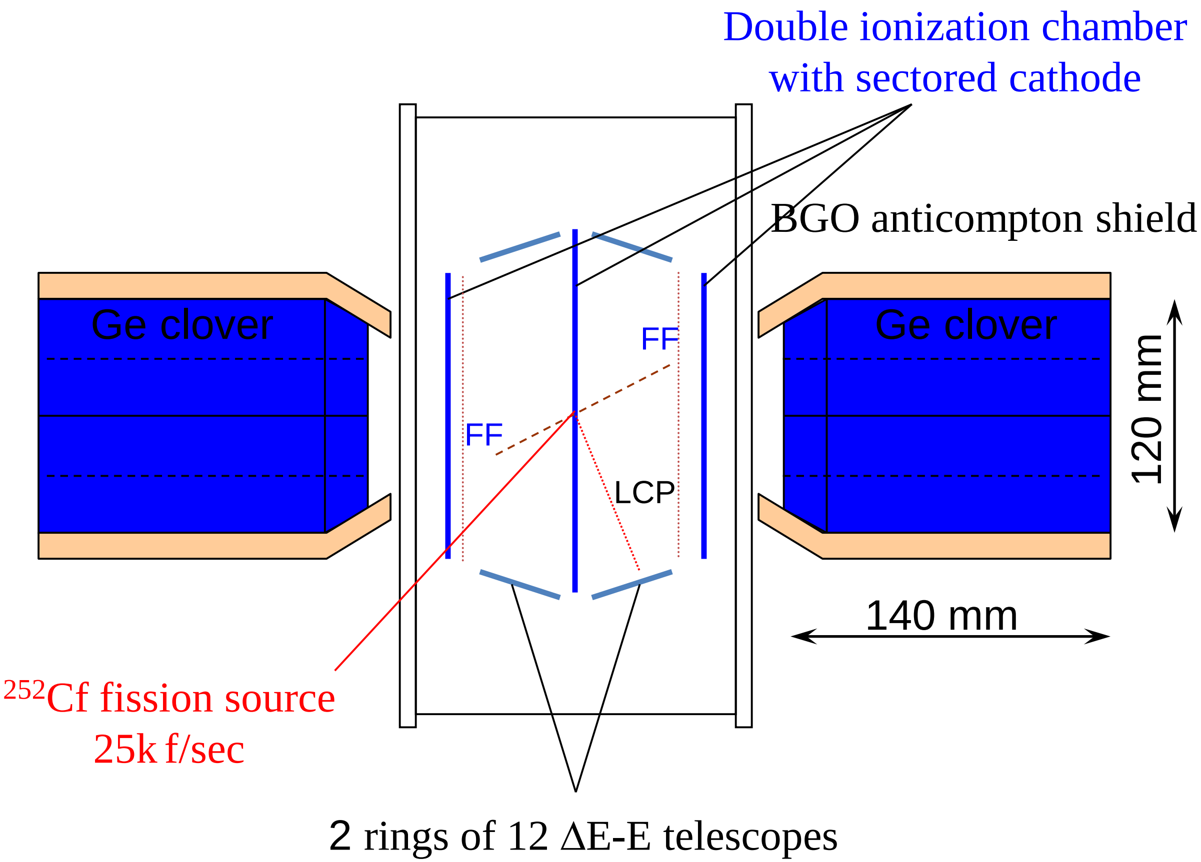

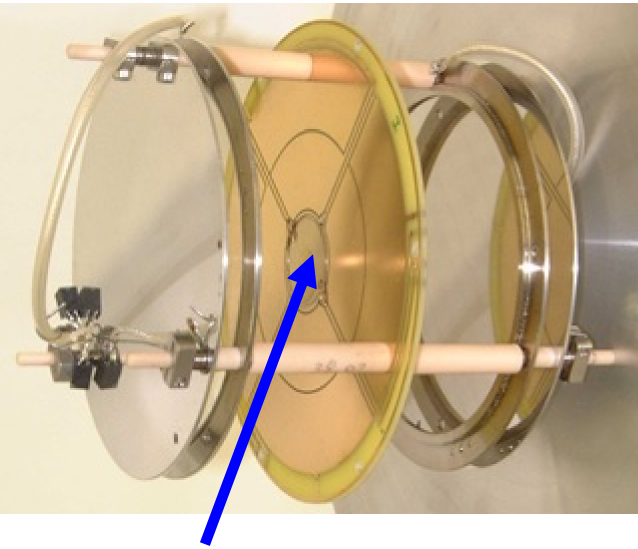

^{252}Cf source (25k f/s)

$T_{1/2}$=2.645y

E_α = 6.118 and 6.076 MeV

bin. fiss./α-decay = 1/31

ter. fiss./α-decay = 1/8308

4π twin ionization chamber for fission fragments

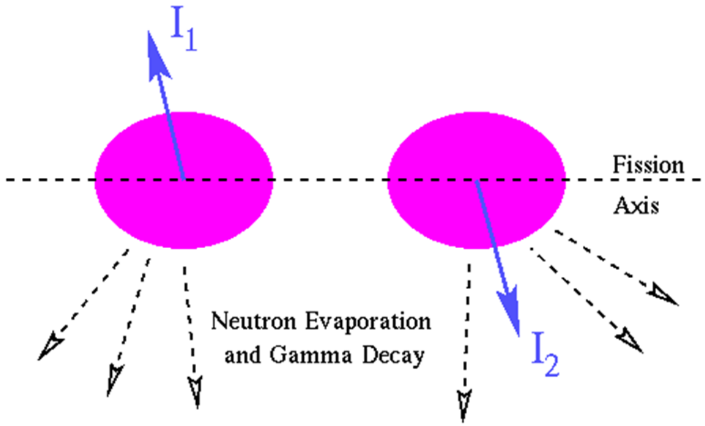

The origin of fragment spins and their alignment

$4^+ \rightarrow 2^+$ transitions

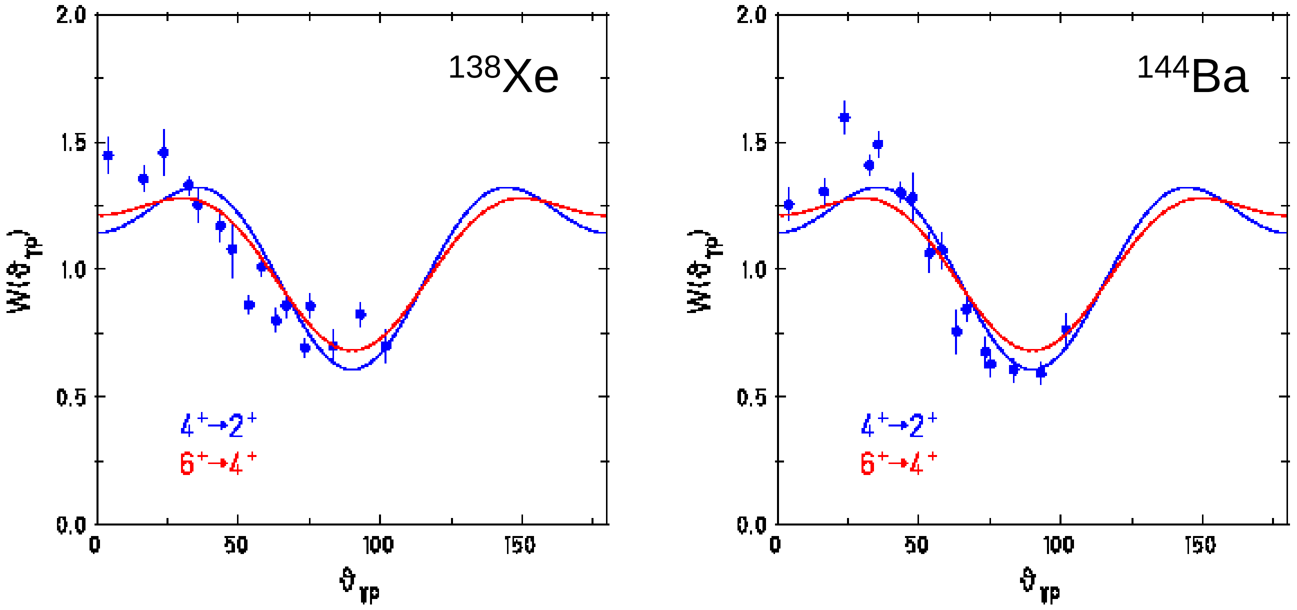

Search for diabolic pair transfer

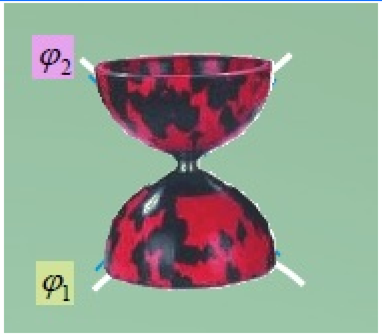

Nuclear Josephson Effects:

Enhanced transfer of nucleon pairs between two superfluid heavy nuclei in a cold reaction correspond to a super-current

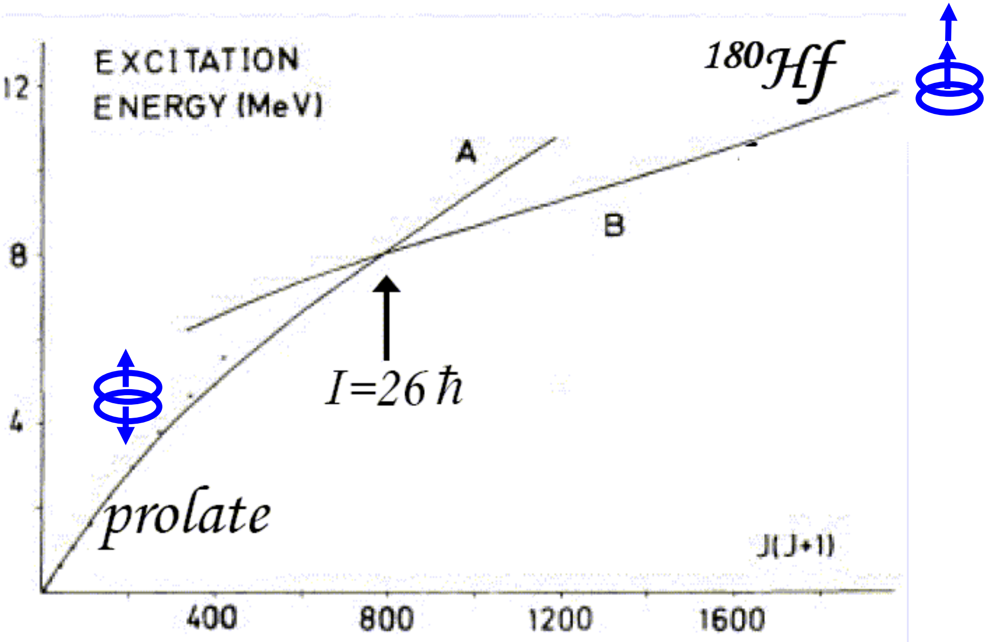

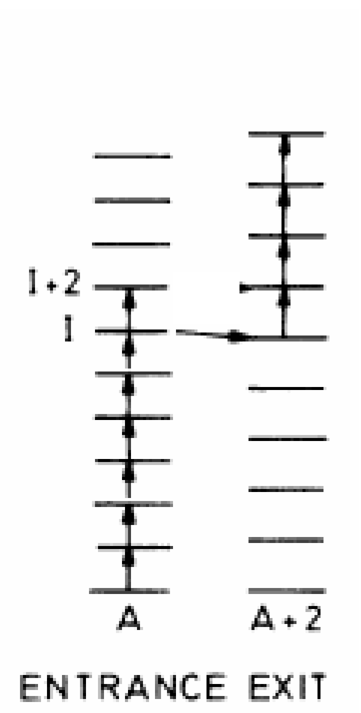

Proposed systems

$^{172,174}Yb$ on ^{206}Pb

$^{174,176}Hf$ on ^{206}Pb

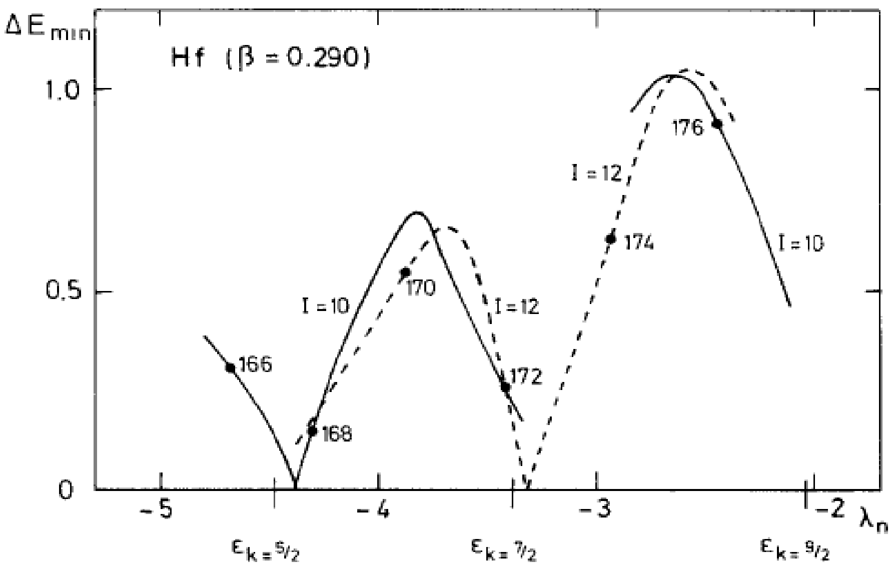

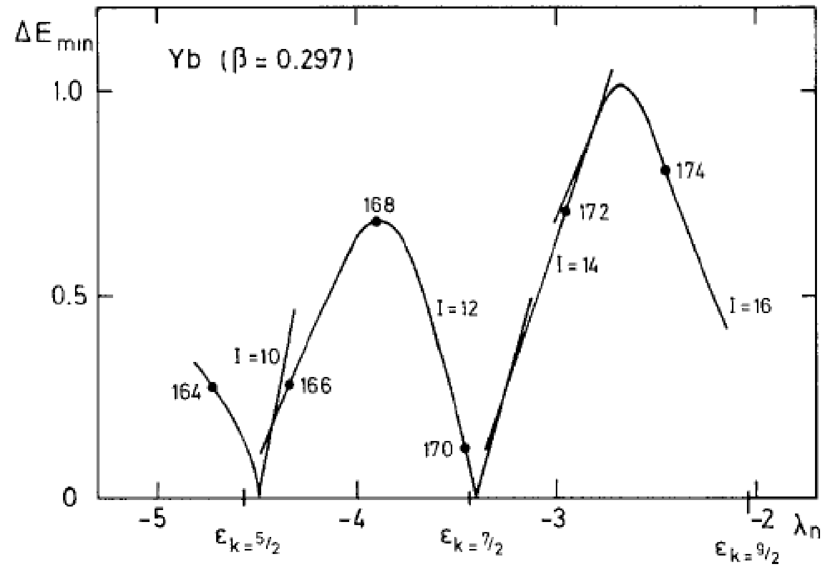

The Hf and Yb-chain : The interaction strength in the level crossing between the ground state band and the s-band characterized by the minimal distance between the yrast band and the first excited band $\Delta E_{min.}$ Connected lines correspond to minimal distances for the angular momenta $I = 10\text{-}16\hbar$. Full dot symbols indicate the even mass Yb-isotopes. The position of the deformed single-particle energies of the $\nu\ i_{13/2}$ levels for the nucleus ^{166}Yb and ^{170}Hf are given on the abscissa.

Y. Sun et al, Z. Phys. A339 (1991) 51

Proposed systems 2n-transfer probability as a function of spin

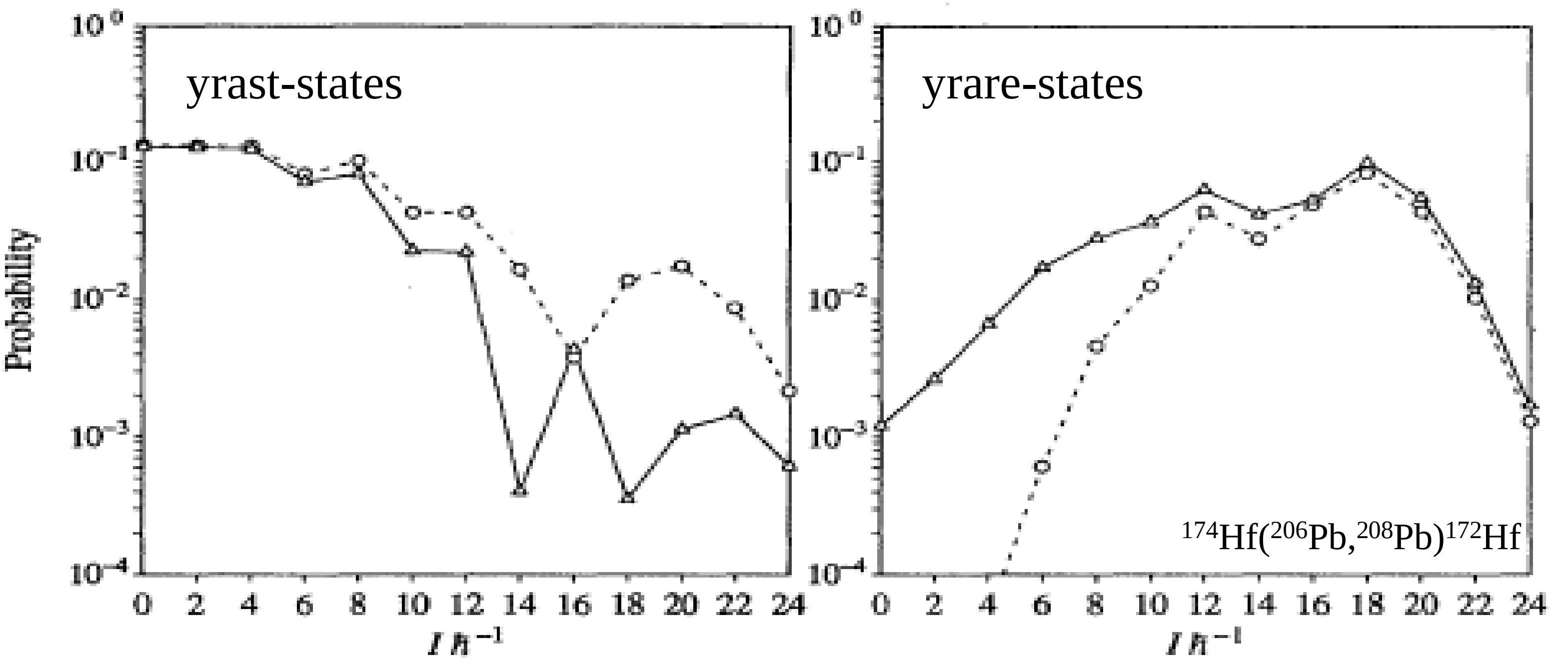

The calculation show the diabolic effect for ^{206}Pb on ^{174}Hf. This calculation assumes ^{174}Hf transfers to ^{172}Hf. The symbol o's are non diabolic case and Δ's are diabolic cases.

L F Canto et al PRC 47,2836(1993).

Open problems

- Coulomb excitation of isomeric states in deformed nuclei
- Nuclear structure of ^{208}Pb
- Studies in the ^{100}Sn region (Magda Gorska)
- Search for diabolic pair transfer at higher angular momentum states

- Mini Orange devices from Johan van Klinken are with Torsten Kröll (TU Darmstadt)

- 10 radioactive targets (0.3 mg/cm^2) from LMU München stored in Mainz (C. Düllmann)
  ^{235}U (1 mg ≡ 80 Bq), ^{237}Np (1 mg ≡ 26 kBq), ^{242}Pu (1 mg ≡ 145 kBq) (area = 0.2 cm^2)
  ^{226}Ra material